Jet Propulsion Laboratory Memorandum IOM 343R-08-003

California Institute of Technology 31-March 2008

The Planetary and Lunar Ephemeris DE 421

W. M. Folkner, J. G. Williams, D. H. Boggs

Abstract

The planetary and lunar ephemeris DE 421 represents the 'current best estimates' of the orbits of the Moon and planets. The lunar orbit is currently known to sub-meter accuracy though fitting lunar laser ranging data. The orbits of Venus, Earth, and Mars areknown to sub-kilometer accuracy. Because of perturbation of the orbit of Mars by asteroids, frequent updates are needed to maintain the current accuracy into the future decade. Mercury's orbit is determined to an accuracy of several kilometers by radar ranging. The orbits of Jupiter and Saturn are determined to accuracies of tens of kilometers as a result of spacecraft tracking and modern ground-based astrometry. The orbits of Uranus, Neptune, and Pluto are not as well determined. Reprocessing of historical observations is expected to lead to improvements in their orbits in the next several years.

1. Introduction

The planetary and lunar ephemeris DE 421 is a significant advance over earlier ephemerides. Compared with DE 418, released in July 2007 (Folkner et al. 2007), the current ephemeris includes additional data, especially range and VLBI measurements of Mars spacecraft; range measurements to the ESA Venus Express spacecraft; and use of current best estimates of planetary masses in the integration process. The lunar orbit is more robust due to an expanded set of lunar geophysical solution parameters, seven additional months of laser ranging data, and complete convergence. DE 421 has been integrated over the time period 1900 to 2050. A longer integration has been deferred until some improvements in the dynamical models have been implemented.

While the lunar orbit in DE 421 is close to that in DE 418, it is a major improvement over the widely distributed DE 405 (Standish 1998). For DE 405 the lunar orbit was not fit in a way consistent with the other planets. Continuing the process used to develop DE 418, DE 421 is a combined fit of lunar laser ranging (LLR) and planetary measurements. The DE 421 model is more complete than for DE 418 and has been fully converged, so it is recommended for use by lunar missions.

Also, DE 405 was created in 1995 before the Mars Pathfinder mission in 1997, so the Earth and Mars orbits were largely dependent on range measurements to the Viking landers from 1976 to 1982 augmented by radar range observations with an accuracy of about 1 km. The error in the Earth and Mars orbits in DE 405, is now known to be about 2 km, which was good accuracy in 1997 but much worse than the current sub-kilometer accuracy.

Because of perturbations of the orbit of Mars by asteroids, frequent updates are needed to maintain the current ephemeris accuracy into the future decade. The orbits of Earth and Mars are continually improved through measurements of spacecraft in orbit about Mars. DE 421 incorporates range data through the end of 2007. VLBI observations of Mars spacecraft were resumed in January 2006 to improve the Mars orbit accuracy for the MSL project. VLBI data through December 2007 have been included in the DE 421 estimate. The Earth and Mars orbit accuracies are expected to be better than 300 m through 2008.

The Venus orbit accuracy has been significantly improved by inclusion of range measurement to the Venus Express spacecraft. Combined with VLBI measurements of Magellan, and one VLBI observation of Venus Express, the Venus orbit accuracy is now about 200 meters.

The orbit of Mercury is currently determined by radar range observations. Since the last radar range point is in 1999, the estimated Mercury orbit has not changed significantly for the past decade. The current orbit accuracy is a few kilometers. Measurements of the Messenger spacecraft are expected to lead to a significant improvement over the next several years.

The orbits of Jupiter and Saturn are determined to accuracies of tens of kilometers using spacecraft tracking and modern ground-based astrometry. The orbit of Saturn is more accurate than that of Jupiter since the Cassini tracking data are more complete and more accurate than previous spacecraft tracking at Jupiter. The orbits of Uranus, Neptune, and Pluto are not as well determined. Reprocessing of historical observations is expected to lead to improvements in their orbits in the next several years.

Below we briefly summarize the dynamical modeling assumptions used in the development of DE 421 and the measurements used in its estimation.

2. Planetary Ephemeris Dynamical Modeling

The time coordinate for DE 421 is consistent with the metric used for integration. The coordinate time has been scaled such that at the location of the Earth the coordinate time has no rate relative to atomic time. In a resolution adopted by the International Astronomical Union in 2006 (GA26.3), the time scale TDB (Temps Dynamique Barycentrique, Barycentric Dynamical Time) was defined to be consistent with the JPL ephemeris time. The conversion from atomic time to coordinate time has been done using the formulation of Fairhead and Bretagnon (1990), updated by Fukushima and Irwin (1999) which is consistent, for planetary navigation accuracies, with the simpler approximation given in Moyer (2000).

The axes of the ephemeris are oriented with respect to the International Celestial Reference Frame (ICRF). The Mars spacecraft VLBI measurements serve to tie the ephemeris to the ICRF with accuracy better than 1 milli-ascsecond (1 mas $\approx$ 5 nanoradian) for the planets with accurate ranges.

For DE 421 the positions of the moon and planets were integrated using a n-body parameterized post-Newtonian metric (Will and Nordtvedt, 1972; Will 1981; Moyer 2000). The PPN parameters γ and β have been set to 1, their values in general relativity. Extended body effects for the Earth-Moon system are described in a companion memo (Williams et al. 2008). The oblateness of the Sun has been modeled with J_2 set to $2.0\text{x}10^{-7}$. Along with the Earth/Moon mass ratio, the mass parameter GM for the Sun, which is by convention a fixed value in units of AU^3/day^2, was estimated in units of km^3/s^2 by solving for the AU in km in the development of DE 421. The mass parameter of the Earth-Moon system was held fixed to a previous LLR-only estimate. The mass parameters for the other planets (planetary systems for planets with natural satellites) were taken from published values derived from spacecraft tracking data. The mass parameters used for the Sun and planets are given in Table 1.

Table1: Mass parameters of planetary bodies/systems used in DE 421

Body/System	GM (km^3/s^2)	GM_{sun}/GM_{planet}	Reference
Mercury	22032.090000	6023597.400017	Anderson et al [1987]
Venus	324858.592000	408523.718655	Konopliv et al. [1999]
Earth	398600.436233	332946.048166	See text
Mars	42828.375214	3098703.590267	Konopliv et al. [2006]
Jupiter	126712764.800000	1047.348625	Jacobson [2005]
Saturn	37940585.200000	3497.901768	Jacobson et al. [2006]
Uranus	5794548.600000	22902.981613	Jacobson et al. [1992]
Neptune	6836535.000000	19412.237346	Jacobson et al. [1991]
Pluto	977.000000	135836683.767599	Jacobson et al. [2007]
Sun	132712440040.944000	1	Estimated
Moon	4902.800076	27068703.185436	See text
Earth-Moon	403503.236310	328900.559150	LLR fit

The orbit of the Sun was not integrated in the same way as the other planets. Instead, the position and velocity of the Sun were derived at each integration time step to keep the solar system barycenter (Estabrook 1971) at the center of the coordinate system.

The Newtonian effects of 67 ‘major’ asteroids and 276 ‘minor’ asteroids that introduce the largest perturbations on the orbit of Mars have been included in the integration of the planetary orbits in an iterative manner. The orbits of Ceres, Pallas, and Vesta were integrated simultaneously, including mutual interactions, holding the orbits of the Sun and planets to those in DE 405. The orbits for the other asteroids were integrated individually under the gravitational forces from the Sun, planets, and Ceres, Pallas and Vesta, whose orbits were held fixed. The mass parameters of Ceres, Pallas, and Vesta, and eight other asteroids were then estimated in fitting the DE 421 data. The mass parameters of the remaining 56 ‘major’ asteroids were held at assumed nominal values. The mass parameters of the major asteroids are given in Appendix A. The minor asteroids were divided into three taxonomic types (classes). The volume of each minor asteroid was based on a nominal radius and the density of each of the three types of asteroids was estimated. The estimated densities and the radii assumed for the minor asteroids are given in Appendix A.

The selection of which asteroid mass parameters to estimate was based on an empirical process to see which set produced a reasonably accurate prediction of the Earth-Mars range over one year. For example, Figure 1 shows Mars Odyssey range residuals relative to DE 418, which was fit to range data through end of 2006. DE 418 is seen to predict range to Mars one year into the future with an accuracy of about 15 m. Similarly DE 421 is expected to predict the Earth-Mars range to about 15 m through end of 2008. (The error in the plane-of-sky position of Mars relative to Earth through end of 2008 is about 300 m.) This is relevant for navigation of the Phoenix spacecraft with arrival at Mars in May 2008. The estimated mass parameters of the selected asteroids and estimated asteroid class densities are not necessarily the best possible values for other purposes.

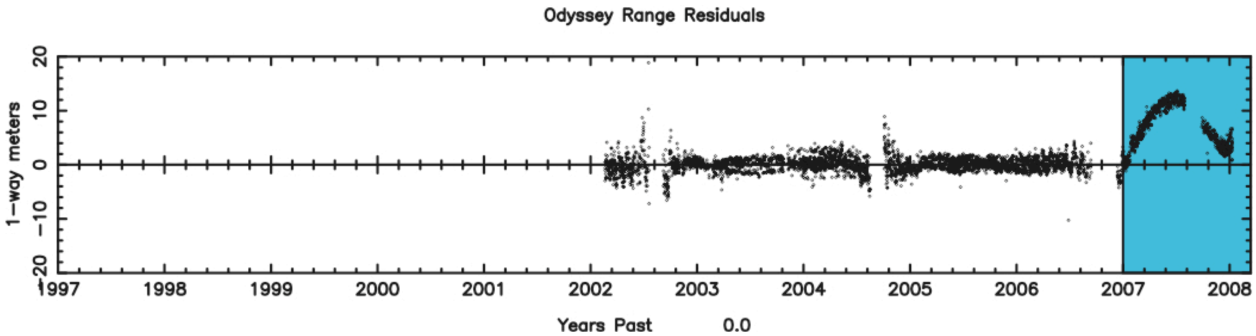

Figure 1: Mars Odyssey spacecraft range measurement residuals to planetary ephemeris DE 418. DE 418 was fit to range measurements through end of 2006. The range residuals for data in 2007 (in shaded area) are less than 15 m and indicate the ephemeris prediction accuracy.

3. Measurement Set

Rather than try to fit all available planetary observations, the data used for DE 421 were preferentially selected for the best accuracy and (for angular data) accuracy of ties to the ICRF. The measurements are summarized in Table 2 and Table 3. Plots of the residuals for all data are included in Appendix B. The data for each planet contain primary data that have the most strength for determining the orbit, and, for some planets, secondary data that are included in the fit at their nominal weight but do not affect the orbit significantly.

Lunar laser ranging, spacecraft ranging, and radar ranging are all very accurate and independent of reference frame. VLBI observations of spacecraft in orbit about Venus, Mars, Jupiter, and Saturn relative to extragalactic radio sources defining the ICRF tie the planetary ephemeris to the ICRF.

Analysis of spacecraft range and Doppler observations taken as spacecraft fly by planets can give right ascension and declination with accuracy somewhat less than the VLBI observations. These right ascension and declination determinations are important in refining the orbits of Jupiter and Saturn. The accuracy of spacecraft plane-of-sky determinations is very much a function of time. The earliest planetary encounters relied on S-band (2 GHz) radio systems with range and Doppler measurement accuracy very sensitive to electrons in the solar plasma. Later spacecraft observations (e.g. after 1990) used X-band (8 GHz) radio systems that were much less affected by solar plasma. Early spacecraft encounter data were processed with reference frame models not well linked to the current ICRF, and often saw discrepancies between range and Doppler data. Data from most encounters have since been re-processed with modern reference frame models so the determined plane-of-sky positions are consistent with the ICRF. For each encounter a single vector for range, right ascension, and declination was generated. For Cassini, a vector was generated for each orbit about Saturn.

Astrometric observations of the planets in the past have suffered from difficulty in establishing an accurate celestial reference frame. Since the release of the Hipparcos star catalog, and the development of techniques for using CCD instruments, astrometric accuracies are approaching spacecraft VLBI accuracies. However these observations only cover a fraction of the orbital periods of the outer planets. Since the orbits of Jupiter and Saturn are well determined from spacecraft data, the limited time span of modern data mainly affects the orbital uncertainties of Uranus, Neptune, and Pluto. The Pluto data set was discussed in detail in relation to the ephemeris DE 418 (Folkner et al. 2007). For the orbit of Pluto in DE421, we followed the same approach used for DE 418, with two more months of observations. For Uranus and Neptune the assessment of older data sets is not as complete as for Pluto so relatively few data have been included. These orbits are reasonably accurate for the current times due to modern astrometry and knowledge from the Voyager encounters. The Uranus and Neptune data sets will be expanded in a future ephemeris.

Most of the data used are not published but communicated to the authors electronically. Most data are available at the web site http://iau-comm4.jpl.nasa.gov/plan-eph-data/ or by request from the authors. Lunar laser ranging data are posted by the International Laser Ranging Service (Pearlman et al 2002; http://ilrs.gsfc.nasa.gov/). A Mariner 10 range to Mercury was reported by Anderson et al. (1987). A Goldstone radar range to Mercury is from Jurgens et al. (1998). Radar ranges to Mercury and Venus from Eupatoria are from Kotelnikov et al (1983; http://www.ipa.nw.ru/PAGE/DEPFUND/LEA/ENG/rrr.html). Astrometry data from the US Naval Observatory are from Stone et al. (2003; http://www.nofs.navy.mil/data/plansat.html). Older observations from Pluto are taken from the literature (see references: Barbieri, Cohen, Jenson, Gemmo, Klemola, Rapaport, Rylkov, Sharaf, Zappala). Other data were via private communications.

4. Availability

The DE421 ephemeris may be downloaded in an ascii version from

ftp://ssd.jpl.nasa.gov/pub/eph/planets/ascii/de421 .

The complete set of input parameters for the solar system integration is part of the file. The SPICE kernal version of DE421 is available at

ftp://ssd.jpl.nasa.gov/pub/eph/planets/bsp .

Table 2: Summary of data used to estimate orbits of the Moon, inner planets and Jupiter. Data with relatively little contribution to the estimates orbits are indicated in italics.

Planet	Meas	Type	Obs	Span	#meas
Moon	LLR	range			
			McDonald 2.7m	1970-1985	3451
			MLRS/saddle	1984-1988	275
			MLRS/MtFowlkes	1988-2007	2746
			Haleakala	1984-1990	694
			CERGA	1984-2005	9177
			Matera	2004	11
			Apache Pt	2006-2007	247
Mercury	Radar	range	Arecibo	1967-1982	242
			Goldstone	1972-1997	283
			Haystack	1966-1971	217
			Eupatoria	1980-1995	75
	Radar	closure	Goldstone	1989-1997	40
	Spacecraft	range	Mariner 10	1974-1975	2
Venus	Spacecraft	range	VEX	2006-2007	14304
	Spacecraft	VLBI	VEX	2007	1
	Spacecraft	VLBI	MGN	1990-1994	18
	Spacecraft	3-D	Cassini	1998-1999	2
	Radar	*range*	*Arecibo*	*1967-1970*	*227*
			Goldstone	*1970-1990*	*512*
			Haystack	*1966-1971*	*229*
			Millstone	*1964-1967*	*101*
			Eupatoria	*1962-1995*	*1134*
Mars	Spacecraft	range	Viking L1	1976-1982	1178
			Viking L2	1976-1977	80
			Pathfinder	1997	90
			MGS	1999-2006	164781
			Odyssey	2002-2007	251999
			MEX	2005-2007	63133
			MRO	2006-2007	7972
	Spacecraft	VLBI	MGS	2001-2003	14
			ODY	2002-2007	66
			MRO	2006-2007	14
Jupiter	Spacecraft	3-D	Pioneer 10	1973	1
			Pioneer 11	1974	1
			Voyager 1	1979	1
			Voyager 2	1979	1
			Ulysses	1992	1
			Cassini	2000	1
	CCD	ra/dec	USNOFS	1998-2007	2533
	Spacecraft	VLBI	Galileo	1996-1997	24
	Transit	*ra/dec*	*Washington*	*1914-1994*	*2053*
			Herstmonceux	*1958-1982*	*468*
			La Palma	*1992-1997*	*658*
			Tokyo	*1986-1988*	*98*
			El Leoncito	*1998*	*11*

Table 3: Summary of data used to estimate orbits of Saturn, Uranus, Neptune, and Pluto. Data with relatively little contribution to the estimates orbits are indicated in italics.

Planet	Meas	Type	Obs	Span	#meas
Saturn	Spacecraft	3-D	Pioneer 11	1979	1
			Voyager 1	1980	1
			Voyager 2	1981	1
			Cassini	2004-2006	31
	CCD	ra/dec	USNOFS	1998-2007	3153
			TMO	2002-2005	778
	Transit	*ra/dec*	*Bordeaux*	*1987-1993*	*119*
			Washington	*1913-1982*	*1422*
			Herstmonceux	*1958-1982*	*405*
			La Palma	*1992-1997*	*730*
			Tokyo	*1986-1988*	*62*
			El Leoncito	*1998*	*18*
Uranus	Spacecraft	3-D	Voyager 2	1986	1
	CCD	ra/dec	USNOFS	1998-2007	1612
			TMO	1998-2007	347
	Transit	ra/dec	Bordeaux	1985-1993	165
			Washington	1914-1993	2043
			Herstmonceux	1957-1981	353
			La Palma	1984-1997	1030
			Tokyo	1986-1988	44
			El Leoncito	1997-1998	8
Neptune	Spacecraft	3-D	Voyager 2	1989	1
	CCD	ra/dec	USNOFS	1998-2007	1588
			TMO	2001-2007	267
	Transit	ra/dec	Bordeaux	1985-1993	348
			Washington	1913-1993	1838
			Herstmonceux	1958-1981	316
			La Palma	1984-1998	1106
			Tokyo	1986-1988	59
			El Leoncito	1998-1999	11
Pluto	CCD	ra/dec	USNOFS	1998-2007	852
			TMO	2001-2007	118
	Photo	ra/dec	misc	1914-1958	42
			Palomar	1963-1965	8
			Pulkovo	1930-1992	53
			Bord/Valin	1995-2001	97
			Asiago	1969-1989	193
			Copenhagen	1975-1978	15
			Lick	1980-1985	11
			Torino	1973-1982	37
	Transit	*ra/dec*	*La Palma*	*1989-1998*	*380*
			El Leoncito	*1999*	*33*

Acknowledgements

The planetary ephemeris accuracy is limited by the accuracy of measurements to which it is fit. The present ephemeris improvements are due to contributed data from many people, including Jim Border for the spacecraft VLBI measurements, Don Han for files used to reduce some of the VLBI measurements, Alex Konopliv for reduced NASA Mars spacecraft ranging measurements, Hugh Harris and Alice Monet at the US Naval Observatory in Flagstaff for observations of the outer planets, Trevor Morely and staff at ESOC for Venus Express and Mars Express range measurements, Bob Jacobson for reduction of Voyager, Pioneer, and Cassini spacecraft tracking data, and Bill Owen for observations of the outer planets from Table Mountain Observatory. Modern lunar laser range quality and quantity are the products of the personnel of the McDonald Observatory in Texas, Apache Point Observatory in New Mexico, Observatoire de la Côte d'Azur in France, and Haleakala Observatory in Hawaii. This work is also greatly dependent on the work of M. Standish, who advised us on aspects of the ephemeris development.

The research described in this paper was carried out at the Jet Propulsion Laboratory, California Institute of Technology, under a contract with the National Aeronautics and Space Administration.

References

Anderson, J. D., Colombo, G., Esposito, P. B., Lau, E. L., Trager, G. B., The mass, gravity field, and ephemeris of Mercury, Icarus, 71, 337-349, 1987.

Barbieri, C., Capaccioli, M., Ganz, R., Pinto, G., Accurate positions of the planet Pluto in the years 1969-1970, Astron. J., 77, 521-522, 1972.

Barbieri, C., Capaccioli, M., Pinto, G., Accurate positions of the planet Pluto in the years 1971-1974, Astron. J., 80, 412-414, 1975.

Barbieri, C., Pinocchio, L., Capacciloi, M., Pinto, G., Schoenmaker, A. A., Accurate positions of the planet Pluto from 1974 to 1978, Astron. J., 84, 1890-1893, 1979.

Barbieri, C., Benacchio, L., Capacciloi, M., Gemmo, A. G., Accurate positions of the planet Pluto from 1979 to 1987", Astron. J., 96, 396-399, 1988.

Cohen, C. J., Hubbard, E. C., Oesterwinter, C., New orbit for Pluto and analysis of differential corrections, Astron. J., 8, 973-988, 1967.

Estabrook, F. B., Derivation of relativistic Lagrangian for n-body equations containing relativity parameters b and g, JPL memo (internal document), 1971.

Fairhead, L.., Bretagnon, P., An analytical formula for the time transformation TB-TT, Astron. Astrophys., 229, 240-247, 1990.

Gemmo, A. G., Barbieri, C, Astrometry of Pluto from 1969 to 1989, Icarus 108, 174-179, 1994.

Folkner, W, M., Standish, E. M., Williams, J. G., Boggs, D., H., Planetary and lunar ephemeris DE418, JPL Memorandum 343R-07-005, 2007.

Fukushima, T. and Irwin A. A., A numerical time ephemeris of the Earth, Astronomy and Astrophysics, 348, 642- 652, 1999.

Jacobson, R. A., Jovian satellite ephemeris JUP230, private communication, 2005.

Jacobson, R. A., The orbits of the satellites of Pluto PLU017, private communication, 2007.

Jacobson, R. A., Riedel, J. E., Taylor, A. H., The orbits of Triton and Nereid from spacecraft and Earth-based observations, Astron. Astrophys., 247, 565-575, 1991.

Jacobson, R. A., Campbell, J. K., Taylor, A. H., Synnott, S. P., The masses of Uranus and its major satellites from Voyager tracking data and Earth-based Uranus satellite data, Astron. J., 103, 2068-2078, 1992.

Jacobson, R. A., Antreasian, P. G., Bordi, J. J., Criddle, K. E., Ionasescu, R., Jones, J. B., Mackenzie, R. A., Pelletier, F. J., Owen, W. M. jr., Roth, D. C., Stauch, J. R., The gravity field of the Saturnian system from satellite observations and spacecraft tracking data, Astron. J., 132, 2520-2526, 2006.

Jensen, K. S., Accurate astrometric positions of Pluto, 1975-1978, Astron. Astrophys. Suppl., 36, 395-398,1979.

Jurgen, R. F., Rojas, F., Slade, M. A., Standish, E. M., Chandler, J. F., Mercury radar ranging data from 1987 to 1997, Astron. J., **116**, 486-488, 1998.

Klemola, A. R., Harlan, E. A., Astrometric observations of the outer planets and minor planets: 1980-1982, Astron. J., 87, 1242-1243, 1982.

Klemola, A. R., Harlan, E. A., Astrometric observations of the outer planets and minor planets: 1982-1983, Astron. J., 89, 879-881, 1984.

Klemola, A. R., Harlan, E. A., Astrometric observations of the outer planets and minor planets: 1984-1985, Astron. J., 92, 195-198, 1986.

Konopliv, A. S., Banerdt, W. B., Sjogren, W. L., Venus gravity: 180^{th} degree and order model, Icarus, 139, 3-18, 1999.

Konopliv, A. S., Yoder, C. F., Standish, E. M., Yuan, D., Sjogren, W. L., A global solution for the Mars static and seasonal gravity, Mars orientation, Phobos and Deimos masses, and Mars ephemeris, Icarus, 182, 23-50, 2006.

Kotelnikov V. A., Alexandrov Y. N., Andreev R. A., Vyshlov A. S., Dubrovin V. M., Zajtsev A. L., Ignatov S. P., Kaevitser V. I., Kozlov A. N., Krymov A. A., Molotov E. P., Petrov G. M., Rzhiga O. N., Tagaevskij A. T., Khasyanov A. F., Shakhovskoj A. M., Shchetinnikov S. A., Radar Observations of Planets, Astronomicheskii Zhurnal, vol. 60, N 3, 1983.

Moyer, T. D., Formulation for observed and computed values of Deep Space Network data types for navigation, Monograph 2, Deep Space Communications and Navigation Series, Jet Propulsion Laboratory/California Institute of Technology, 2000.

Pearlman, M.R., Degnan, J.J., and Bosworth, J.M., The International Laser Ranging Service, Advances in Space Research, Vol. 30, No. 2, pp. 135-143, July 2002, DOI:10.1016/S0273-1177(02)00277-6.

Rapaport, M., Teixeira, R., Le Campion, J. F., Ducourant, C., Camargo, J. I. B., Benevides-Soares, P., Astrometry of Pluto and Saturn with the CCD meridian instruments of Bordeaux and Valinhos, Astron. Astrophys., 383, 1054-1061, 2002.

Rylkov, V. P., Vityazev, V. V., Dementieva, A. A., Pluto: an analysis of photographic positions obtained with the Pulkovo normal astrograph in 1930-1992, Astronomical and Astrophysical Transactions, vol. 6, pp. 251-281, 1995.

Sharaf. Sh. G., Budnikova. N. A., Theory of the motion of the planet Pluto, Trans. Inst. Theoretical Astronomy, 10, 1-173, 1964 (NASA Technical Translation F-491, 1969).

Standish, E. M., JPL Planetary and lunar ephemeris DE405/LE405, JPL Interoffice Memorandum 312.F-98-04, 1998.

Stone, R. C., Monet, D. G., Monet A. K. B., Harris, F. H, Ables, H. D., Dahn, C. C., Canzian, B., Guetter, H. H., Harris, H. C., Henden, A. A., Levine, S. E., Luginbuhl, C. B., Munn, J. A., Pier, J. R., Vrba. F. J., Walker, R. L., Upgrades to the Flagstaff astrometric scanning transit telescope: a fully automated telescope for astrometry, Astron. J., 126, 2060-2080, 2003.

Will, C. M. and Nordtvedt, K., Conservation laws and preferred frames in relativistic gravity. I. Preferred-frame theories and an extended PPN formalism, Astrophys. J., 177, 757-774, 1972.

Will, C. M., Theory and Experiment in Gravitational Physics, Cambridge University Press, 1981.

Williams, J. G., Boggs, D. H., Folkner, W. M., DE421 Lunar Orbit, Physical Librations, and Surface Coordinates, JPL Interoffice Memorandum 335-JW,DB,WF-20080314-001, March 14, 2008.

Zappala, V., de Sanctis, G., Ferreri, W., Astrometric observations of Pluto from 1973 to 1979, Astron. Astrophys. Suppl., 41, 29-31, 1980.

Zappala, V., de Sanctis, G., Ferreri, W., Astrometric positions of Pluto from 1980 to 1982, Astron. Astrophys. Suppl., 51, 385-387, 1983.

Appendix A: Asteroid Parameters

Table A1: Parameters of 'major' asteroids: type; radius r in km; mass parameter GM in km^3/s^2; density ρ in gm/cm^3.

ID	Name	r	Type	GM	ρ
1	Ceres	474.0	G	62.178	2.1
2	Pallas	266.0	B	13.402	2.5
3	Juno	117.0	Sk	1.536	3.4
4	Vesta	265.0	V	17.630	3.4
5	Astraea	59.5	S	0.159	2.7
6	Hebe	92.6	S	0.605	2.7
7	Iris	99.9	S	0.796	2.9
8	Flora	67.9	S	0.236	2.7
9	Metis	95.0	S	0.567	2.4
10	Hygiea	203.6	C	5.364	2.3
11	Parthenope	77.7	S	0.356	2.7
13	Egeria	103.8	C	0.412	1.3
14	Irene	76.0	S	0.348	2.8
15	Eunomia	127.7	S	1.638	2.8
16	Psyche	126.6	M	2.233	3.9
18	Melpomene	70.3	S	0.267	2.7
19	Fortuna	100.0	Ch	0.463	1.7
20	Massalia	72.8	S	0.291	2.7
21	Lutetia	47.9	M	0.139	4.5
22	Kalliope	90.5	M	0.491	2.4
23	Thalia	53.8	S	0.129	3.0
24	Themis	99.0	C	0.403	1.5
25	Phocaea	37.6	S	0.040	2.7
27	Euterpe	48.0	S	0.084	2.7
28	Bellona	60.5	S	0.165	2.7
29	Amphitrite	106.1	S	0.906	2.7
30	Urania	49.8	S	0.095	2.7
31	Euphrosyne	128.0	C	1.139	1.9
41	Daphne	87.0	Ch	0.527	2.9
42	Isis	50.1	S	0.092	2.6
45	Eugenia	107.3	C	0.397	1.2
51	Nemausa	73.9	C	0.144	1.3
52	Europa	151.3	C	1.354	1.4
60	Echo	30.1	S	0.021	2.7
63	Ausonia	51.6	S	0.102	2.7
65	Cybele	118.6	C	0.694	1.5
69	Hesperia	69.1	M	0.414	4.5
78	Diana	60.3	C	0.085	1.4
94	Aurora	102.4	C	0.414	1.4
97	Klotho	41.4	M	0.089	4.5
98	Ianthe	52.2	C	0.055	1.4
105	Artemis	59.5	C	0.088	1.5
111	Ate	67.3	C	0.116	1.4
135	Hertha	39.6	M	0.078	4.5
139	Juewa	78.3	C	0.188	1.4
145	Adeona	75.6	C	0.151	1.3
187	Lamberta	65.6	C	0.105	1.3
192	Nausikaa	51.6	S	0.107	2.8
194	Prokne	84.2	C	0.182	1.1
216	Kleopatra	62.0	M	0.299	4.5
230	Athamantis	54.5	S	0.126	2.8
324	Bamberga	114.5	CP	0.661	1.6
337	Devosa	29.6	M	0.033	4.5
344	Desiderata	66.1	C	0.114	1.4
354	Eleonora	77.6	Sl	0.327	2.5
372	Palma	94.3	C	0.355	1.5
405	Thia	62.5	C	0.092	1.4
409	Aspasia	80.8	C	0.216	1.5
419	Aurelia	64.5	C	0.102	1.4
451	Patientia	112.5	C	0.610	1.5
488	Kreusa	75.1	C	0.164	1.4
511	Davida	163.0	C	1.638	1.4
532	Herculina	111.1	S	0.886	2.3
554	Peraga	47.9	C	0.044	1.4
654	Zelinda	63.7	Ch	0.090	1.2
704	Interamnia	158.3	C	2.464	2.2
747	Winchester	85.9	C	0.196	1.1

Table A2: Estimated densities ρ in gm/cm^3 of 'minor' asteroids

Type	ρ
C	1.093
S	3.452
M	4.221

Table A3: Parameters of ‘minor’ asteroids: type and radius r in km.
(Continued on next page.)

ID	Name	Type	r
326	Tamara	C	46.5
328	Gudrun	S	61.5
329	Svea	C	38.9
334	Chicago	C	77.9
335	Roberta	C	44.5
336	Lacadiera	C	34.6
338	Budrosa	M	31.6
345	Tercidina	C	47.1
346	Hermentari	S	53.3
347	Pariana	M	25.6
349	Dembowska	S	69.9
350	Ornamenta	C	59.2
356	Liguria	C	65.7
357	Ninina	C	53.0
358	Apollonia	C	44.7
360	Carlova	C	57.9
362	Havnia	C	49.0
363	Padua	C	48.5
365	Corduba	C	53.0
366	Vincentina	C	46.9
369	Aeria	M	30.0
373	Melusina	C	47.9
375	Ursula	C	108.0
377	Campania	C	45.5
381	Myrrha	C	60.3
385	Ilmatar	S	45.8
386	Siegena	C	82.5
387	Aquitania	S	50.3
388	Charybdis	C	57.1
389	Industria	S	39.5
393	Lampetia	C	48.4
404	Arsinoe	C	48.8
407	Arachne	C	47.5
410	Chloris	C	61.8
412	Elisabetha	C	45.5
415	Palatia	C	38.2
416	Vaticana	S	42.7
420	Bertholda	C	70.6
423	Diotima	C	104.4
424	Gratia	C	43.6
426	Hippo	C	63.5
431	Nephele	C	47.5
432	Pythia	S	23.4
433	Eros	S	9.7
442	Eichsfeldi	C	32.9
444	Gyptis	C	79.8

ID	Name	Type	r
445	Edna	C	43.6
449	Hamburga	C	42.8
454	Mathesis	C	40.8
455	Bruchsalia	C	42.2
464	Megaira	C	37.0
465	Alekto	C	36.7
466	Tisiphone	C	57.8
469	Argentina	C	62.8
471	Papagena	S	67.1
476	Hedwig	C	58.4
481	Emita	C	116.0
485	Genua	S	31.9
489	Comacina	C	69.7
490	Veritas	C	57.8
491	Carina	C	48.7
498	Tokio	C	41.4
503	Evelyn	C	40.8
505	Cava	C	57.5
506	Marion	C	53.0
508	Princetonia	C	71.2
514	Armida	C	53.1
516	Amherstia	M	36.5
517	Edith	M	45.6
521	Brixia	C	57.8
535	Montague	C	37.2
536	Merapi	C	75.7
545	Messalina	C	55.6
547	Praxedis	M	34.8
566	Stereoskopi	C	84.1
568	Cheruskia	C	43.5
569	Misa	C	36.5
584	Semiramis	S	27.0
585	Bilkis	C	29.1
591	Irmgard	M	25.9
593	Titania	C	37.7
595	Polyxena	C	54.5
596	Scheila	C	56.7
598	Octavia	C	36.2
599	Luisa	S	32.4
602	Marianna	C	62.4
604	Tekmessa	M	32.6
618	Elfriede	C	60.1
623	Chimaera	C	22.1
626	Notburga	C	50.4
635	Vundtia	C	49.1
663	Gerlinde	C	50.4

ID	Name	Type	r
667	Denise	C	40.6
674	Rachele	S	48.7
675	Ludmilla	S	38.0
680	Genoveva	C	42.0
683	Lanzia	C	41.0
690	Wratislavi	C	67.5
691	Lehigh	C	43.8
694	Ekard	C	45.4
696	Leonora	C	37.9
702	Alauda	C	97.4
705	Erminia	C	67.1
709	Fringilla	C	48.3
712	Boliviana	C	63.8
713	Luscinia	C	52.8
735	Marghanna	C	37.2
739	Mandeville	C	53.7
740	Cantabia	C	45.4
751	Faina	C	55.3
752	Sulamitis	M	31.4
760	Massinga	S	35.6
762	Pulcova	C	68.5
769	Tatjana	C	53.2
772	Tanete	C	58.8
773	Irmintraud	C	47.9
776	Berbericia	C	75.6
778	Theobalda	C	32.0
780	Armenia	C	47.2
784	Pickeringi	C	44.7
786	Bredichina	C	45.8
788	Hohenstein	C	51.8
790	Pretoria	C	85.2
791	Ani	C	51.8
804	Hispania	C	78.6
814	Tauris	C	54.8
849	Ara	M	30.9
895	Helio	C	71.0
909	Ulla	C	58.2
914	Palisana	C	38.3
980	Anacostia	S	43.1
1015	Christa	C	48.5
1021	Flammario	C	49.7
1036	Ganymed	S	15.8
1093	Freda	C	58.4
1107	Lictoria	M	39.6
1171	Rusthaweli	C	35.1
1467	Mashona	C	112.0

Table A3 (continued): Parameters of ‘minor’ asteroids: type and radius r in km.

ID	Name	Type	r	ID	Name	Type	r	ID	Name	Type	r
326	Tamara	C	46.5	445	Edna	C	43.6	667	Denise	C	40.6
328	Gudrun	S	61.5	449	Hamburga	C	42.8	674	Rachele	S	48.7
329	Svea	C	38.9	454	Mathesis	C	40.8	675	Ludmilla	S	38.0
334	Chicago	C	77.9	455	Bruchsalia	C	42.2	680	Genoveva	C	42.0
335	Roberta	C	44.5	464	Megaira	C	37.0	683	Lanzia	C	41.0
336	Lacadiera	C	34.6	465	Alekto	C	36.7	690	Wratislavi	C	67.5
338	Budrosa	M	31.6	466	Tisiphone	C	57.8	691	Lehigh	C	43.8
345	Tercidina	C	47.1	469	Argentina	C	62.8	694	Ekard	C	45.4
346	Hermentari	S	53.3	471	Papagena	S	67.1	696	Leonora	C	37.9
347	Pariana	M	25.6	476	Hedwig	C	58.4	702	Alauda	C	97.4
349	Dembowska	S	69.9	481	Emita	C	116.0	705	Erminia	C	67.1
350	Ornamenta	C	59.2	485	Genua	S	31.9	709	Fringilla	C	48.3
356	Liguria	C	65.7	489	Comacina	C	69.7	712	Boliviana	C	63.8
357	Ninina	C	53.0	490	Veritas	C	57.8	713	Luscinia	C	52.8
358	Apollonia	C	44.7	491	Carina	C	48.7	735	Marghanna	C	37.2
360	Carlova	C	57.9	498	Tokio	C	41.4	739	Mandeville	C	53.7
362	Havnia	C	49.0	503	Evelyn	C	40.8	740	Cantabia	C	45.4
363	Padua	C	48.5	505	Cava	C	57.5	751	Faina	C	55.3
365	Corduba	C	53.0	506	Marion	C	53.0	752	Sulamitis	M	31.4
366	Vincentina	C	46.9	508	Princetonia	C	71.2	760	Massinga	S	35.6
369	Aeria	M	30.0	514	Armida	C	53.1	762	Pulcova	C	68.5
373	Melusina	C	47.9	516	Amherstia	M	36.5	769	Tatjana	C	53.2
375	Ursula	C	108.0	517	Edith	M	45.6	772	Tanete	C	58.8
377	Campania	C	45.5	521	Brixia	C	57.8	773	Irmintraud	C	47.9
381	Myrrha	C	60.3	535	Montague	C	37.2	776	Berbericia	C	75.6
385	Ilmatar	S	45.8	536	Merapi	C	75.7	778	Theobalda	C	32.0
386	Siegena	C	82.5	545	Messalina	C	55.6	780	Armenia	C	47.2
387	Aquitania	S	50.3	547	Praxedis	M	34.8	784	Pickeringi	C	44.7
388	Charybdis	C	57.1	566	Stereoskopia	C	84.1	786	Bredichina	C	45.8
389	Industria	S	39.5	568	Cheruskia	C	43.5	788	Hohenstein	C	51.8
393	Lampetia	C	48.4	569	Misa	C	36.5	790	Pretoria	C	85.2
404	Arsinoe	C	48.8	584	Semiramis	S	27.0	791	Ani	C	51.8
407	Arachne	C	47.5	585	Bilkis	C	29.1	804	Hispania	C	78.6
410	Chloris	C	61.8	591	Irmgard	M	25.9	814	Tauris	C	54.8
412	Elisabetha	C	45.5	593	Titania	C	37.7	849	Ara	M	30.9
415	Palatia	C	38.2	595	Polyxena	C	54.5	895	Helio	C	71.0
416	Vaticana	S	42.7	596	Scheila	C	56.7	909	Ulla	C	58.2
420	Bertholda	C	70.6	598	Octavia	C	36.2	914	Palisana	C	38.3
423	Diotima	C	104.4	599	Luisa	S	32.4	980	Anacostia	S	43.1
424	Gratia	C	43.6	602	Marianna	C	62.4	1015	Christa	C	48.5
426	Hippo	C	63.5	604	Tekmessa	M	32.6	1021	Flammario	C	49.7
431	Nephele	C	47.5	618	Elfriede	C	60.1	1036	Ganymed	S	15.8
432	Pythia	S	23.4	623	Chimaera	C	22.1	1093	Freda	C	58.4
433	Eros	S	9.7	626	Notburga	C	50.4	1107	Lictoria	M	39.6
442	Eichsfeldi	C	32.9	635	Vundtia	C	49.1	1171	Rusthaweli	C	35.1
444	Gyptis	C	79.8	663	Gerlinde	C	50.4	1467	Mashona	C	112.0

Appendix B. Measurement Residual Plots

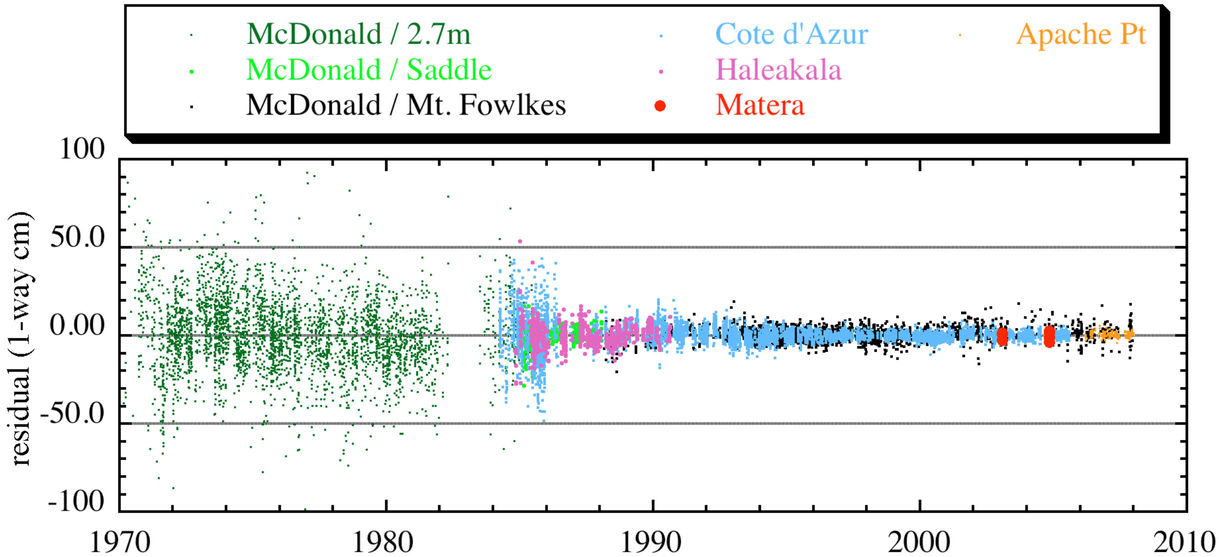

Figure B-1: Lunar laser ranging residuals.

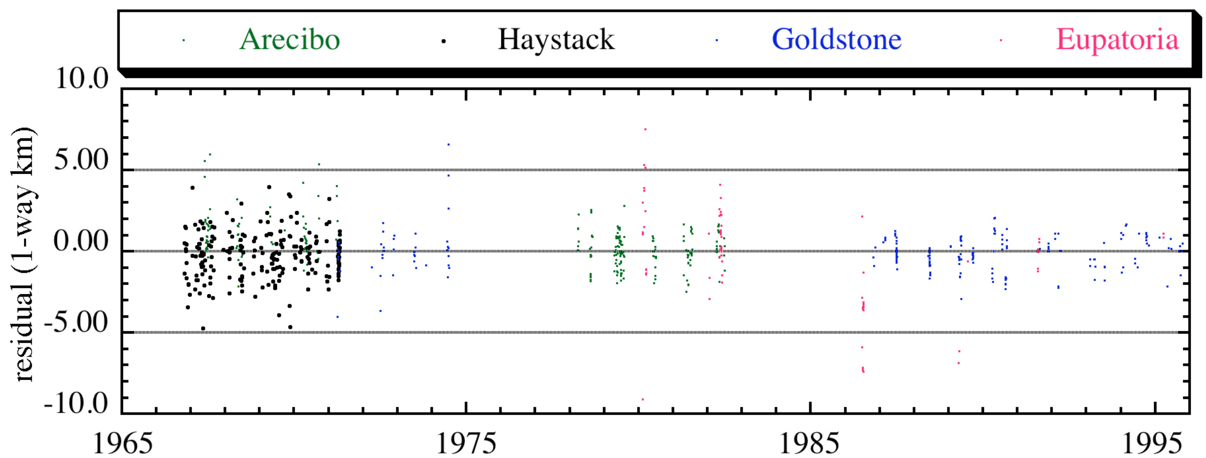

Figure B-2: Mercury radar range residuals.

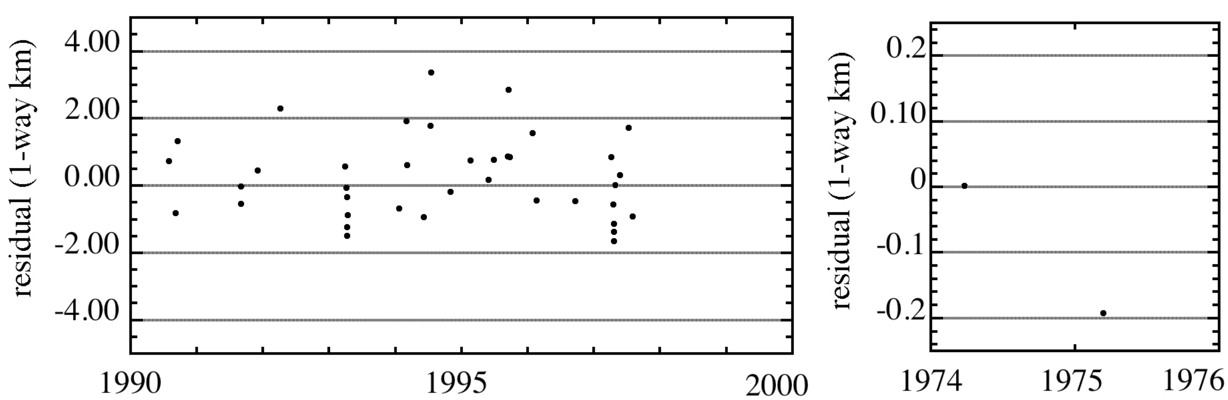

Figure B-3: a) Mercury radar closure residuals. b) Mariner 10 range residuals at Mercury

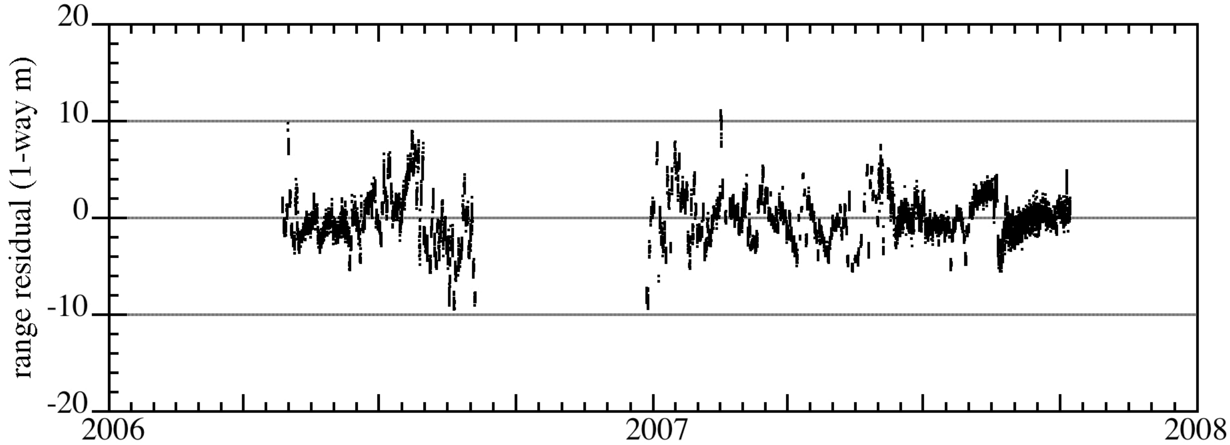

Figure B-4: Venus Express range residuals.

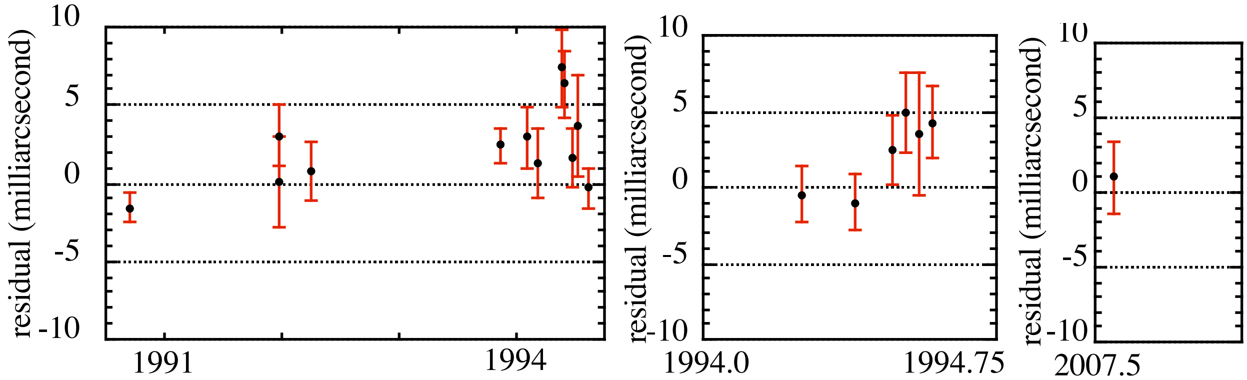

Figure B-5: Venus spacecraft VLBI residuals: a) Magellan from Goldstone-Canberra baseline; b) Magellan from Goldstone-Madrid baseline; c) Venus Express from Goldstone-Madrid baseline.

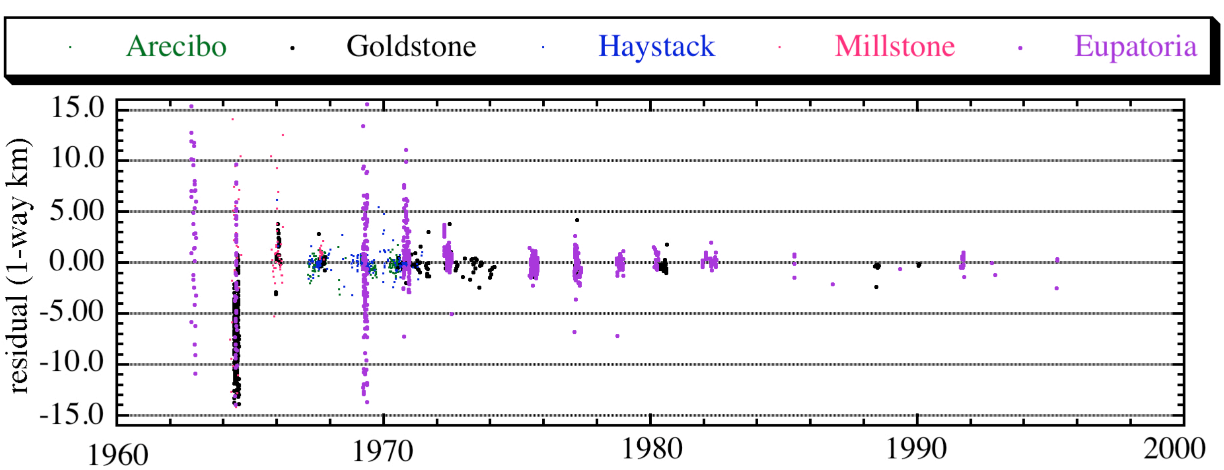

Figure B-6: Venus radar range residuals.

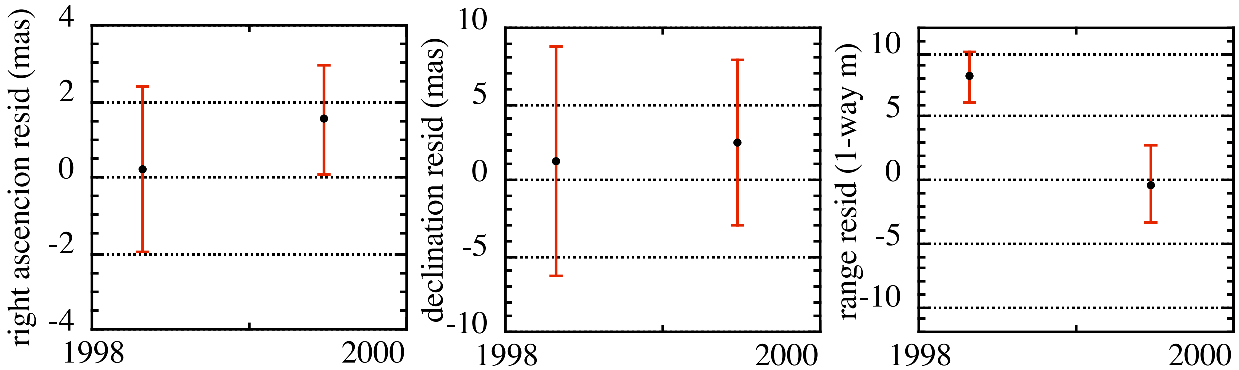

Figure B-7: Residuals for Cassini encounters at Venus.

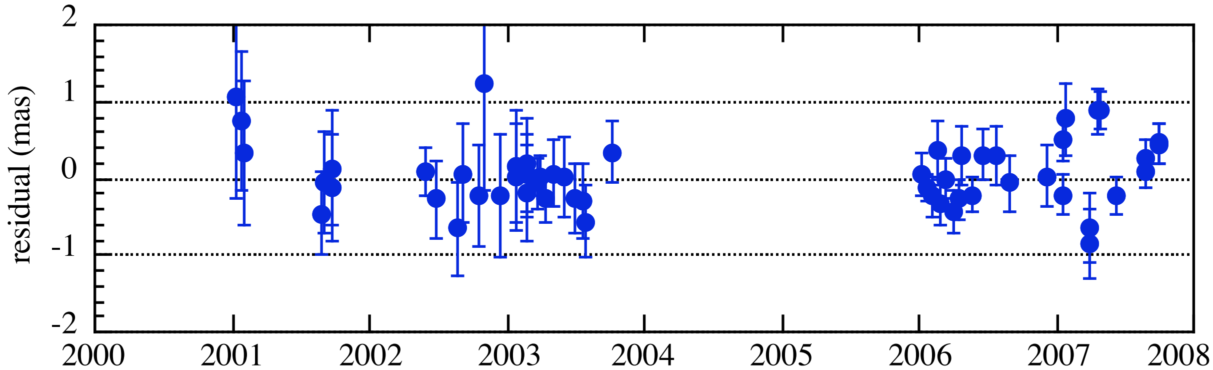

Figure B-8: Residuals for Mars spacecraft VLBI on Goldstone-Canberra baseline.

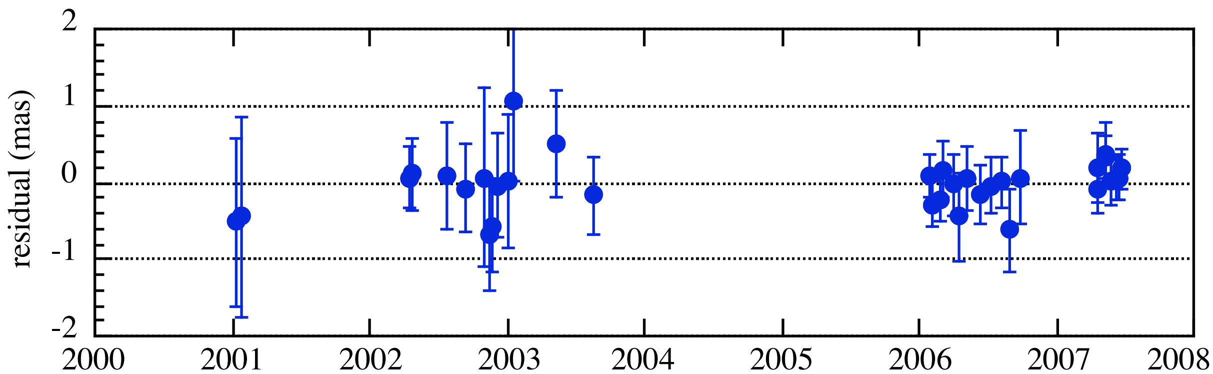

Figure B-9: Residuals for Mars spacecraft VLBI on Goldstone-Madrid baseline.

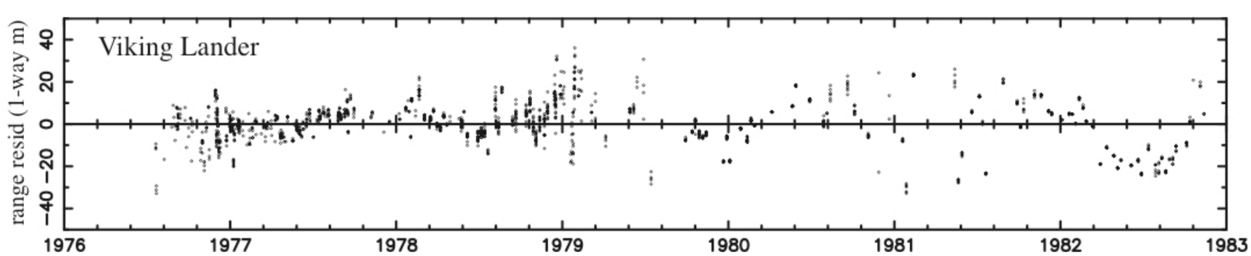

Figure B-10: Viking Lander range residuals.

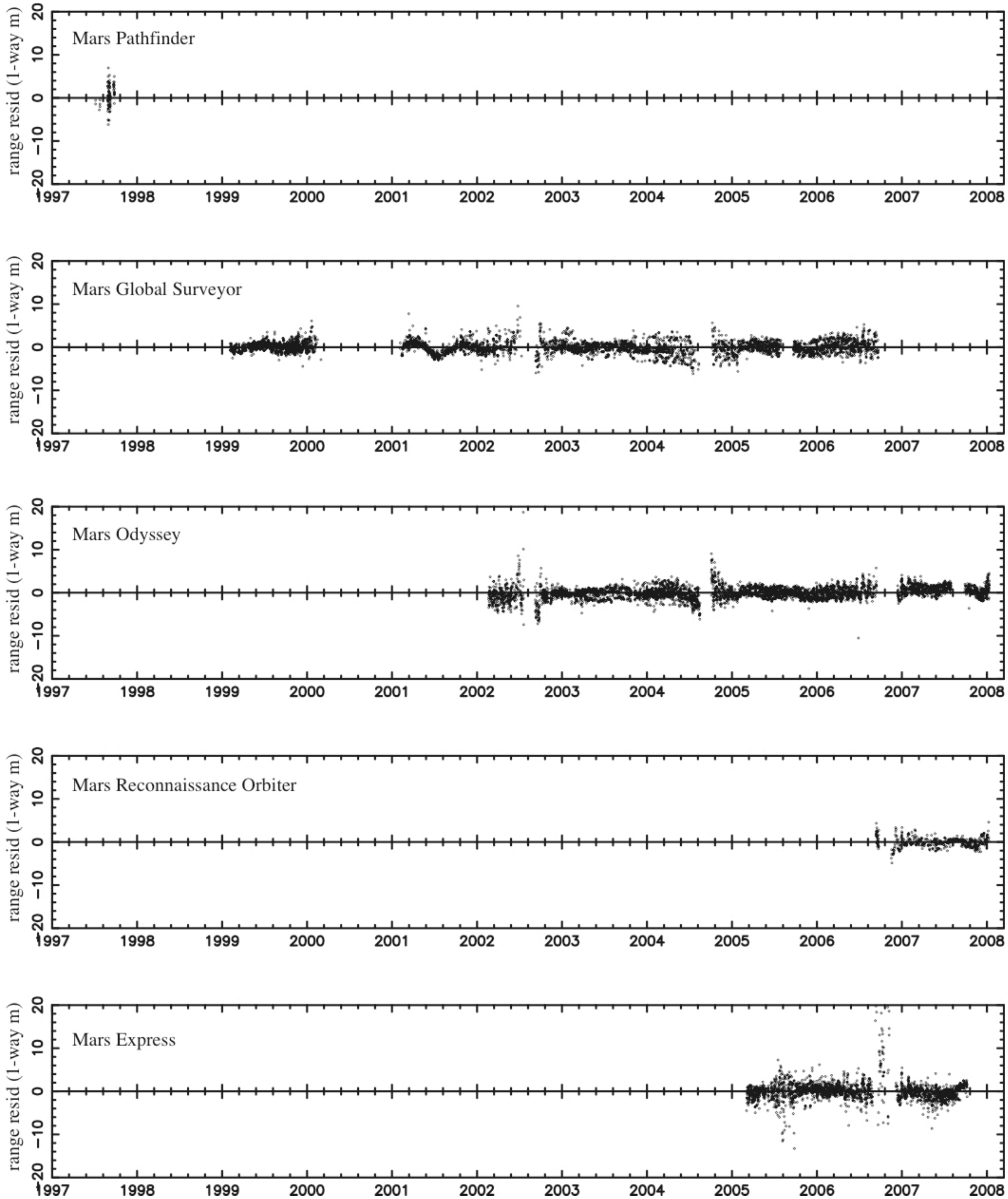

Figure B-11: Post-Viking Mars spacecraft range residuals.

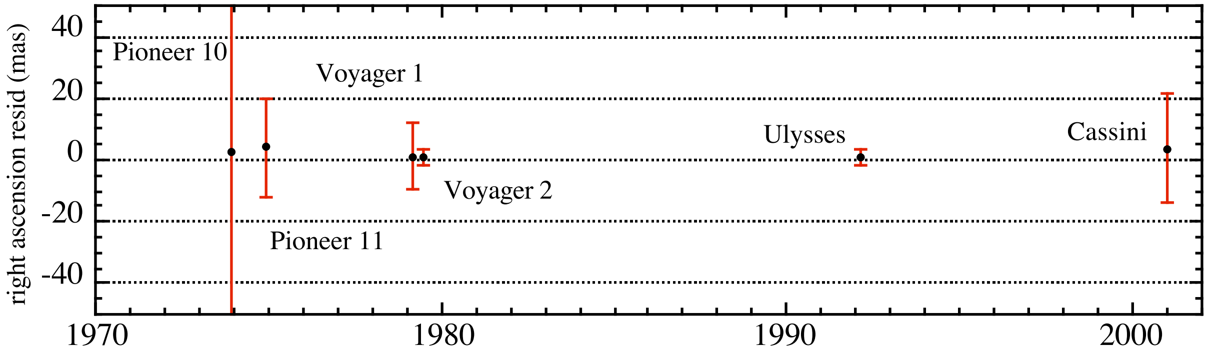

Figure B-12: Jupiter right ascension from spacecraft encounters.

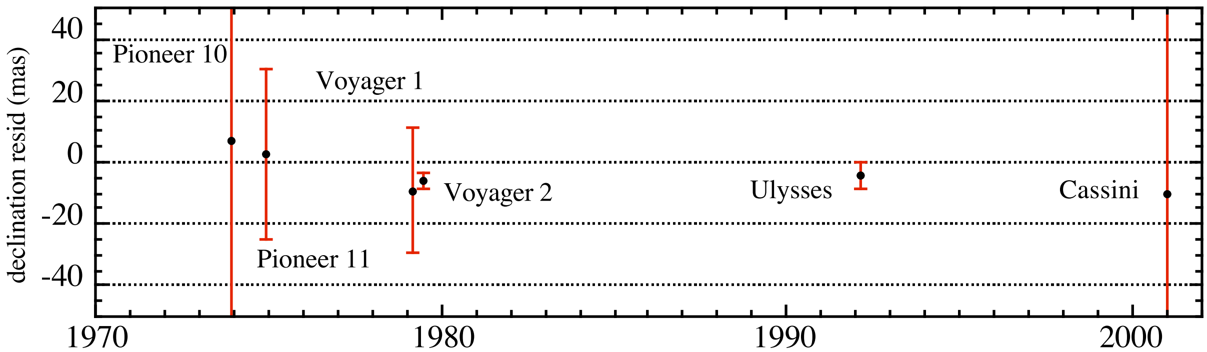

Figure B-13: Jupiter declination from spacecraft encounters.

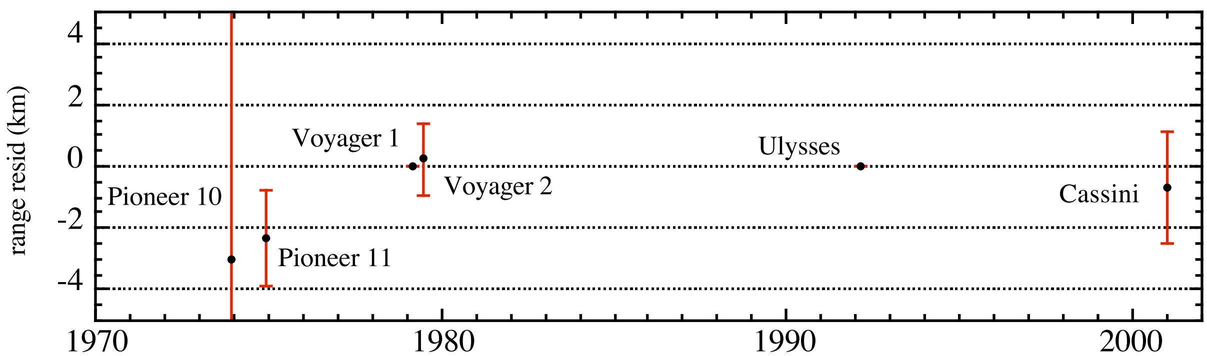

Figure B-14: Earth-Jupiter range from spacecraft encounters.

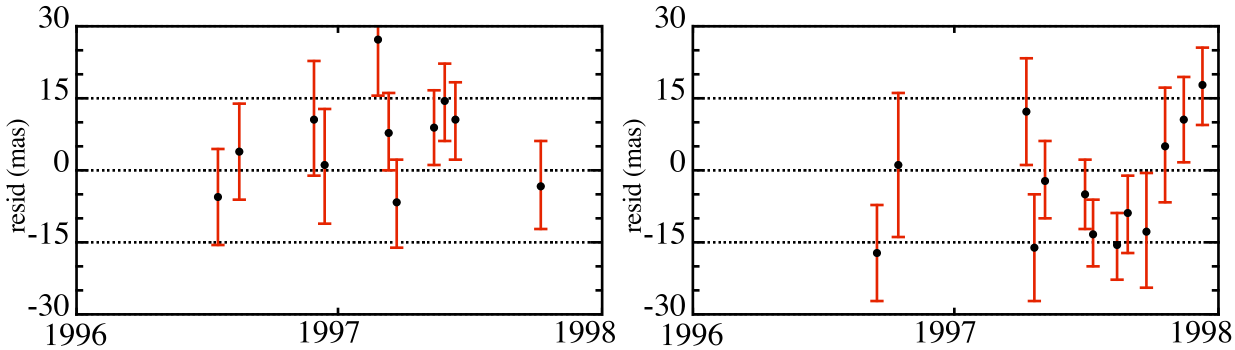

Figure B-15: VLBI observations of Galileo at Jupiter on a) Goldstone-Canberra baseline and b) Goldstone-Madrid baseline.

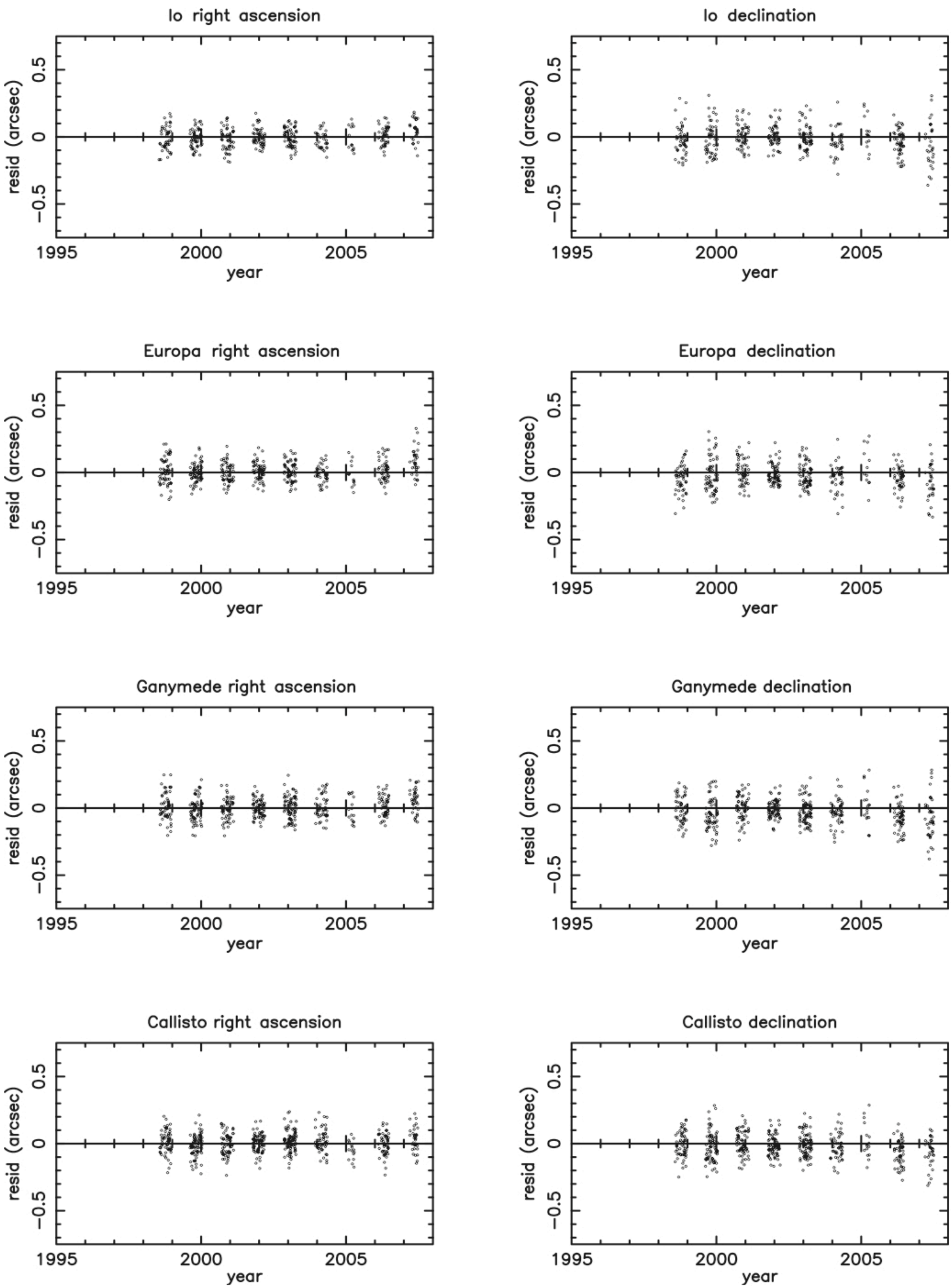

Figure B-16: Observations of Galilean satellites from US Naval Observatory, Flagstaff.

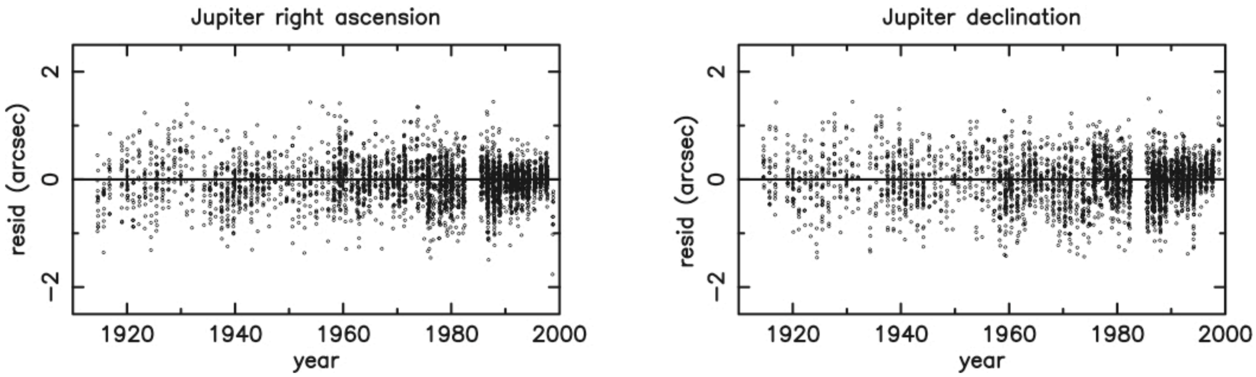

Figure B-17: Transit observations of Jupiter

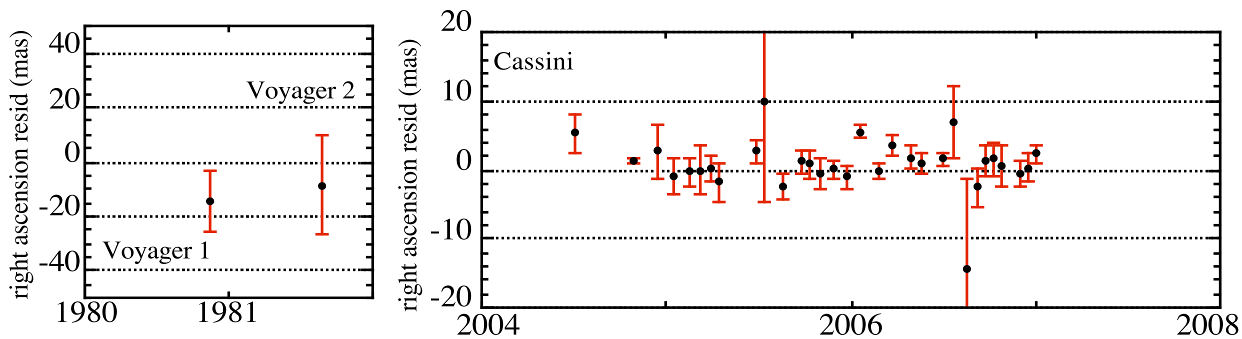

Figure B-18: Saturn right ascension from Voyage 1&2 and Cassini tracking analysis.

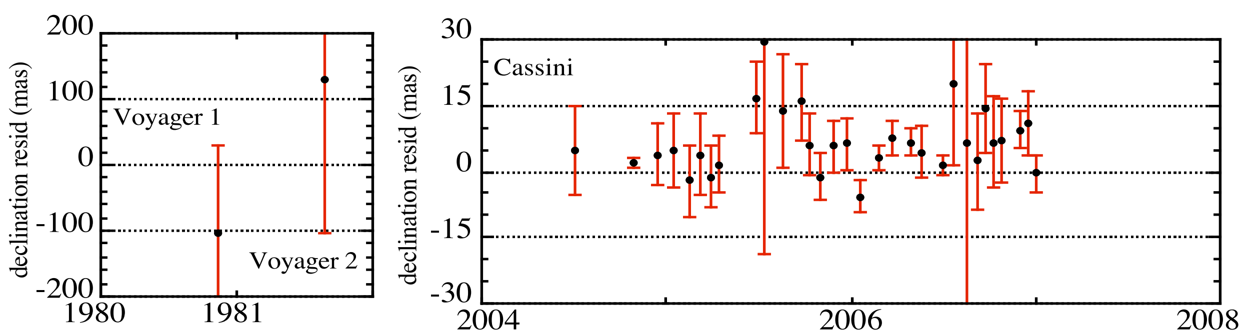

Figure B-19: Saturn declination from spacecraft encounters.

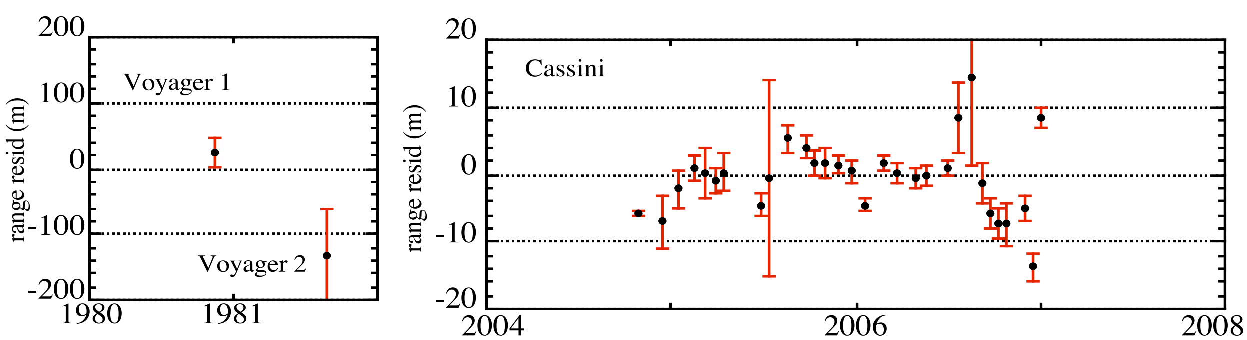

Figure B-20: Saturn-Earth range from spacecraft encounters.

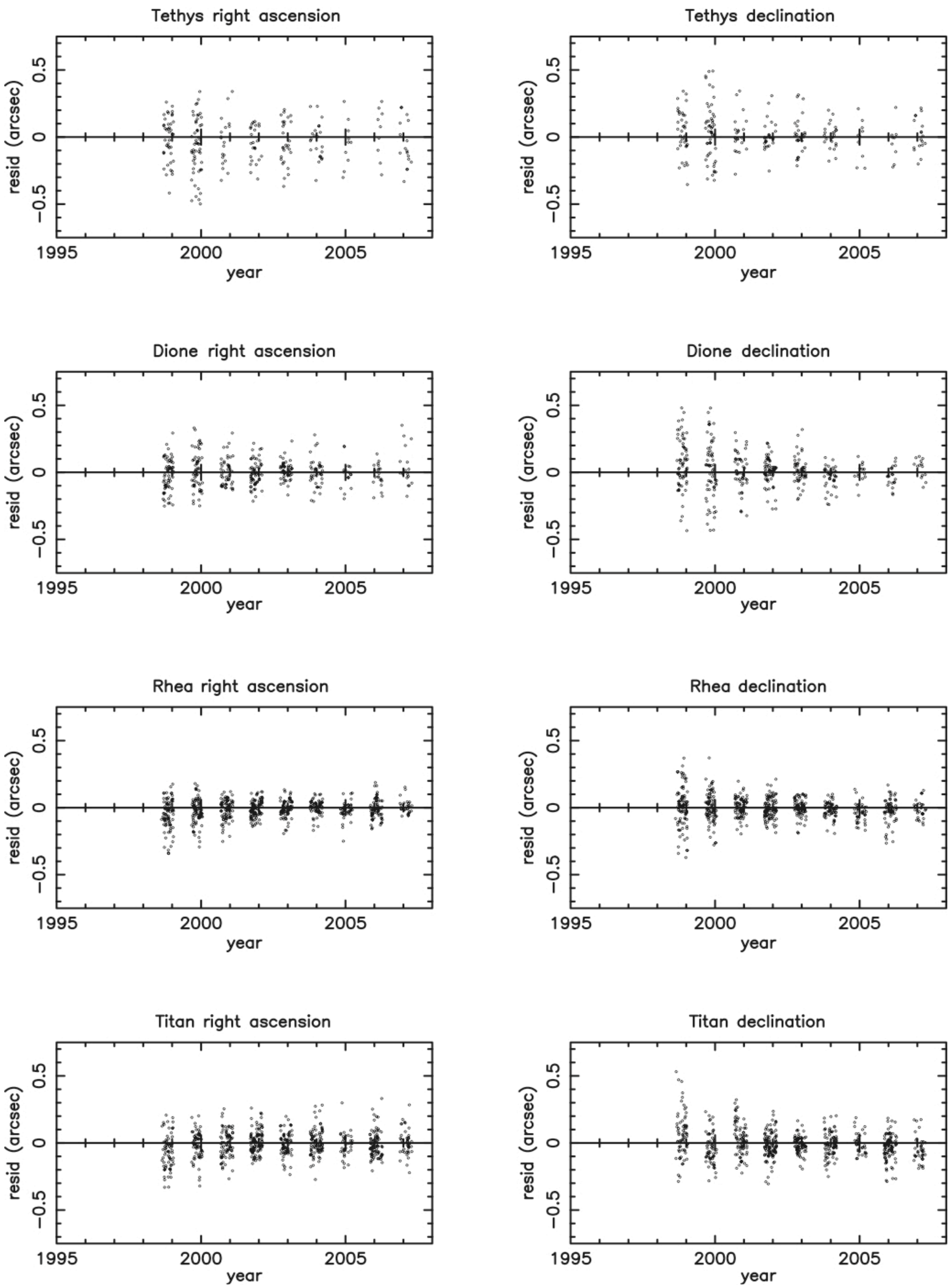

Figure B-21: Saturn satellite (3-6) observations from US Naval Observatory, Flagstaff.

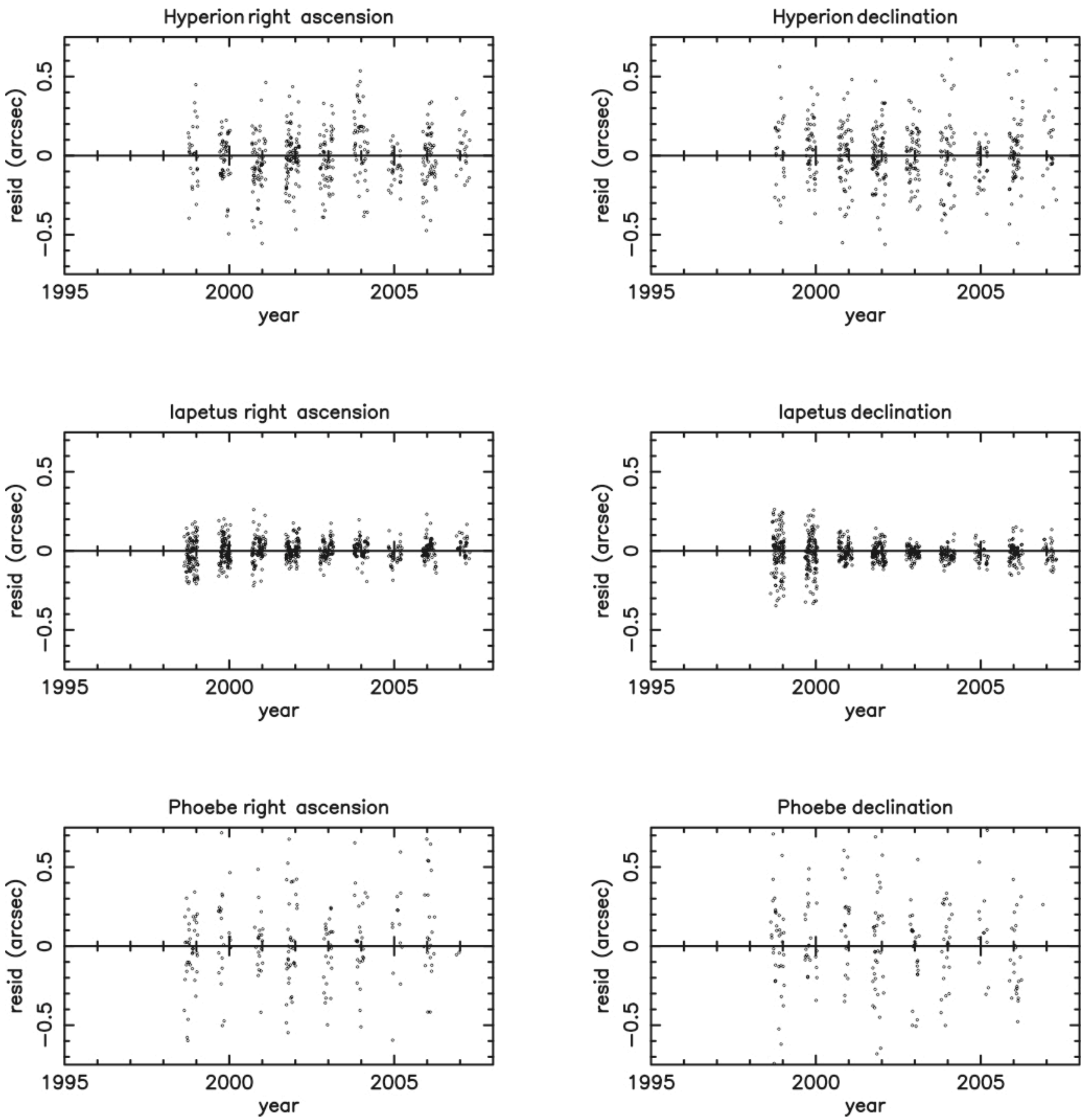

Figure B-22: Saturn satellite (7-9) observations from US Naval Observatory, Flagstaff.

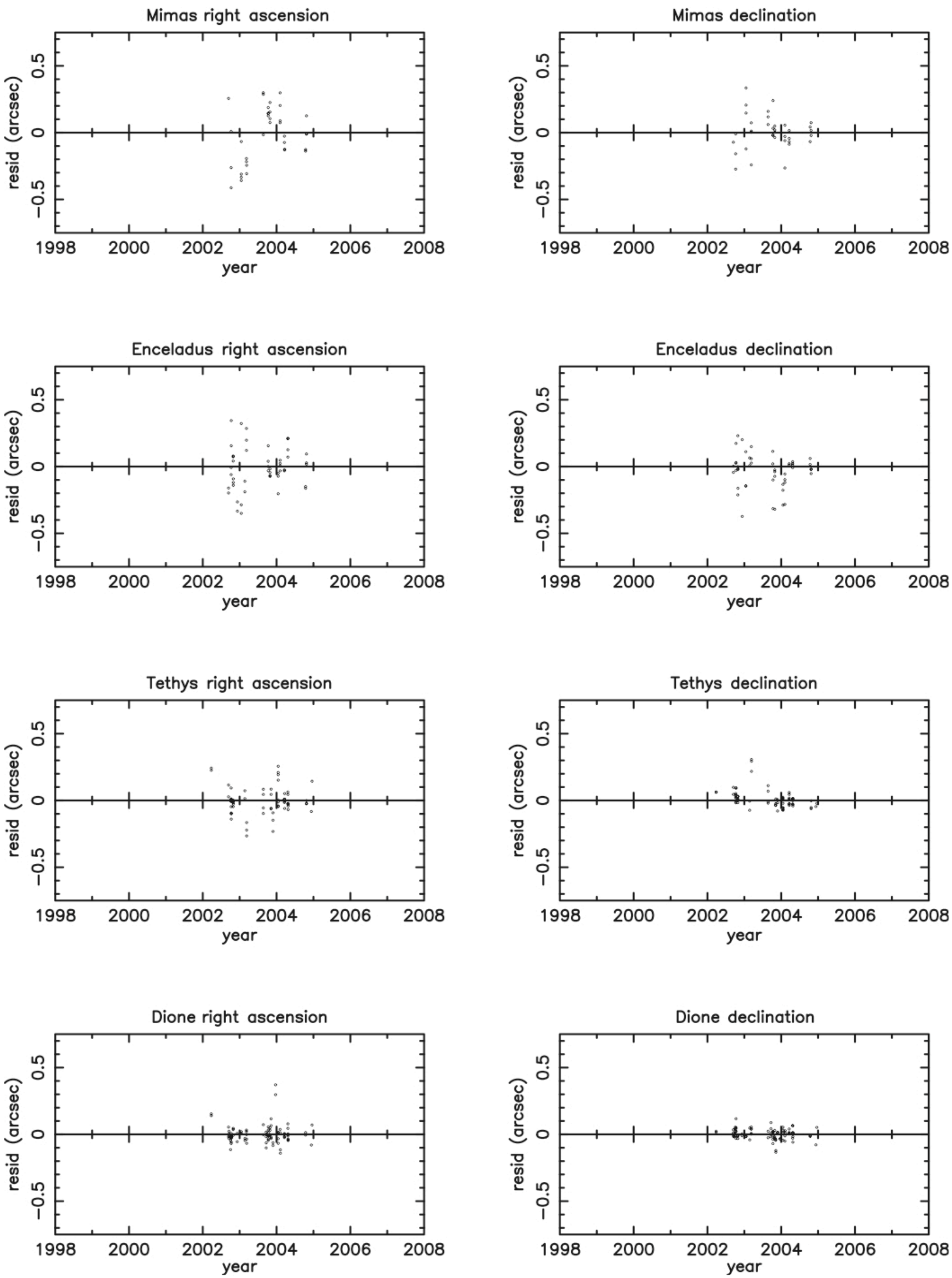

Figure B-23: Saturn satellite (1-4) observations from Table Mountain Observatory.

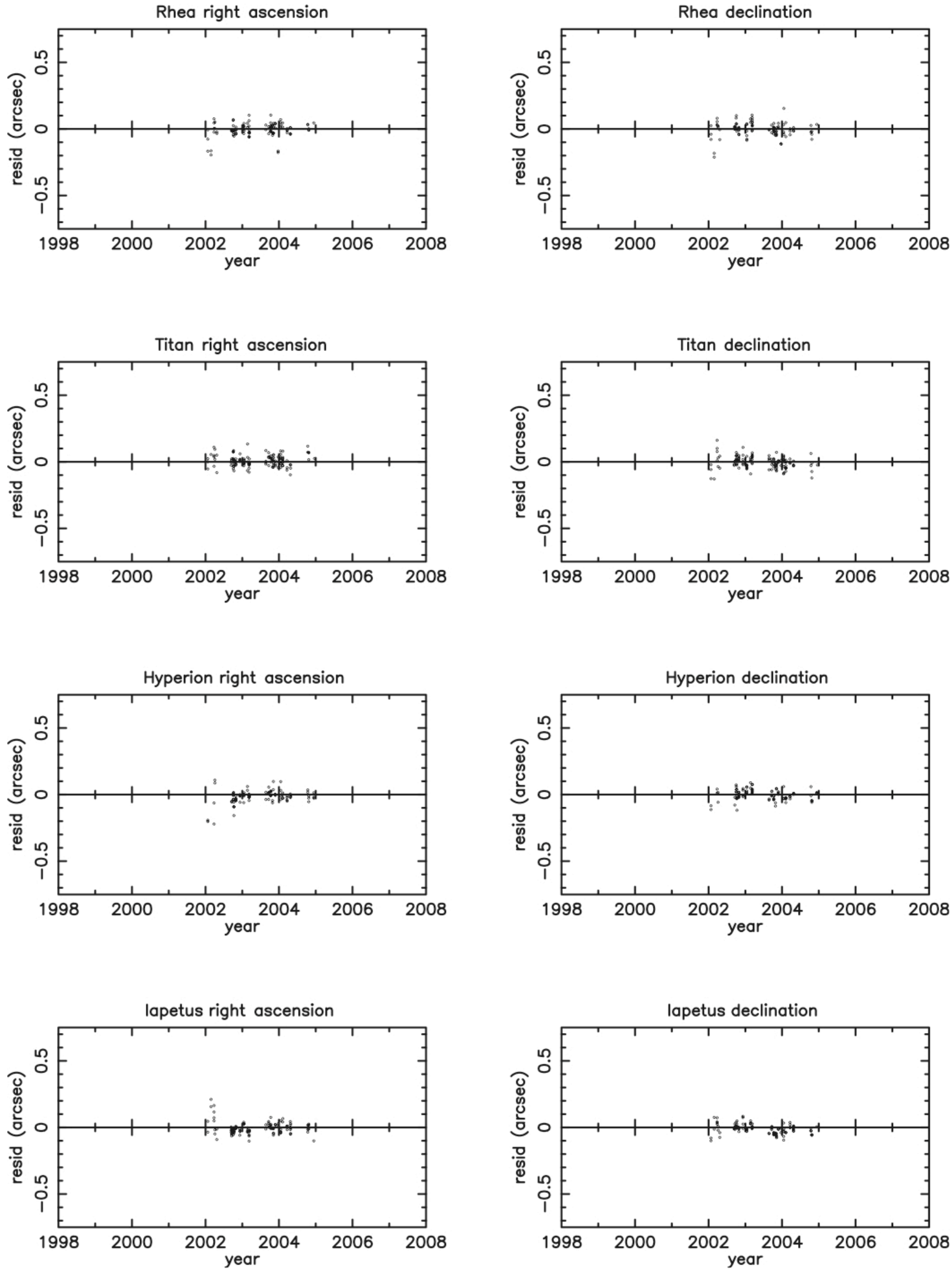

Figure B-24: Saturn satellite (5-8) observations from Table Mountain Observatory.

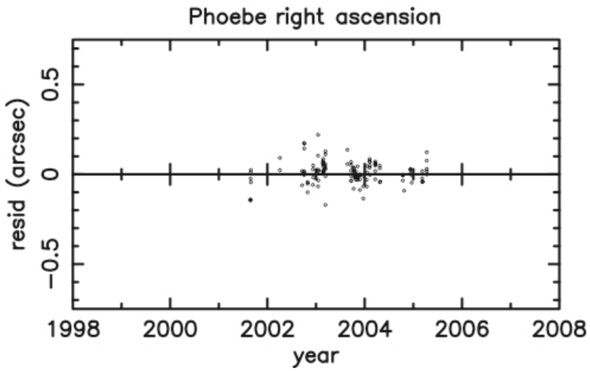

Figure B-25: Saturn satellite (9) observations from Table Mountain Observatory.

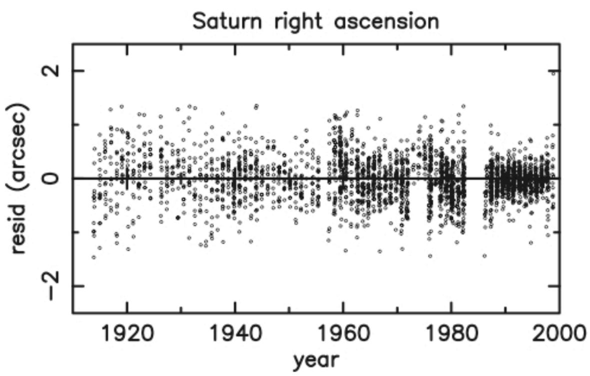

Figure B-26: Transit observations of Saturn

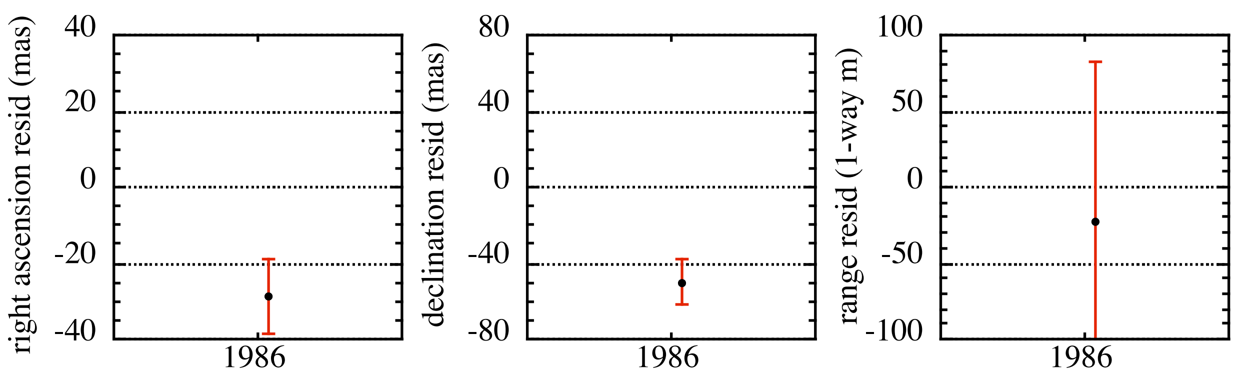

Figure B-27: Uranus right ascension, declination, and range from Voyager 2 encounter.

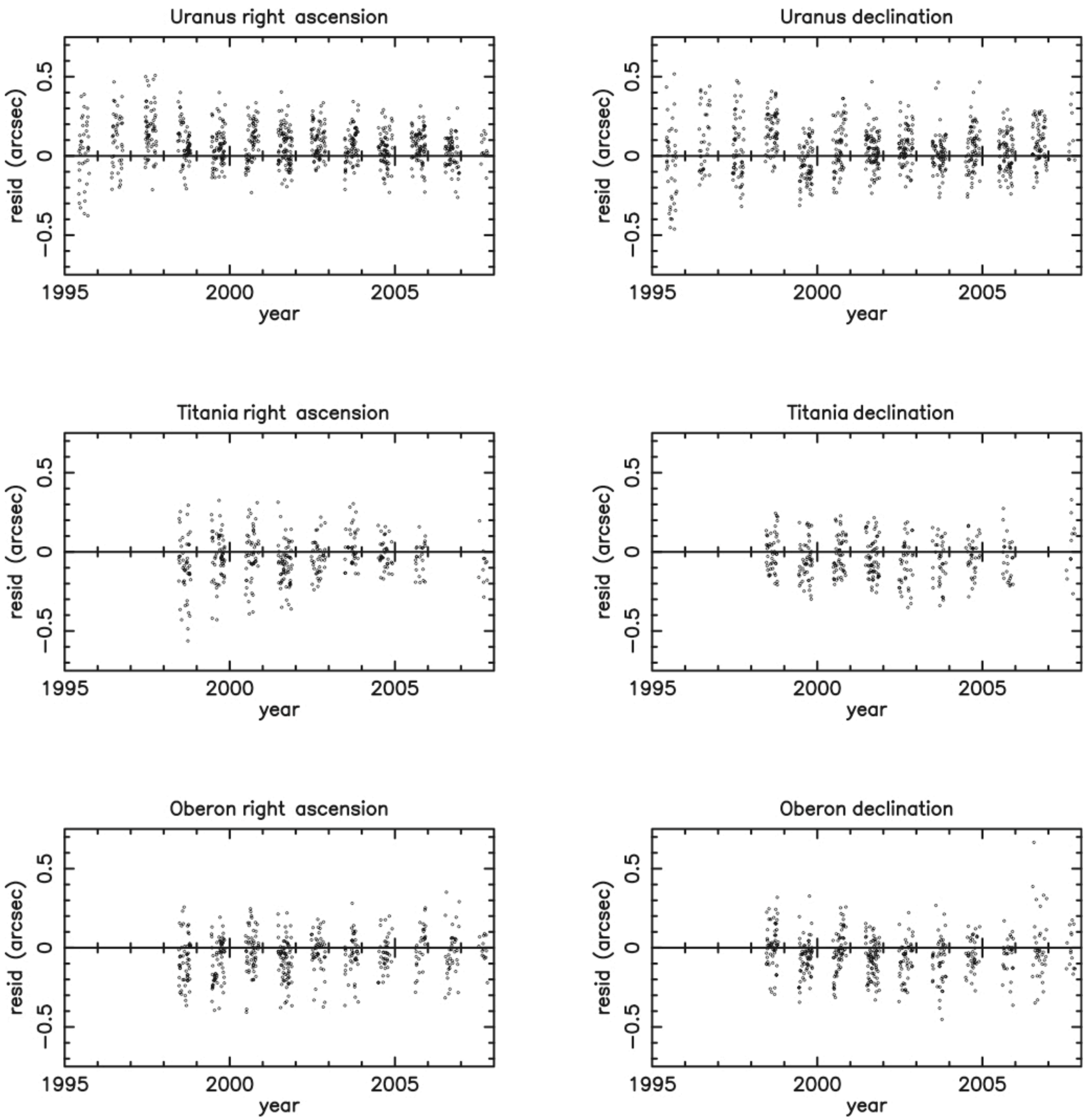

Figure B-28: Uranus observations from US Naval Observatory, Flagstaff.

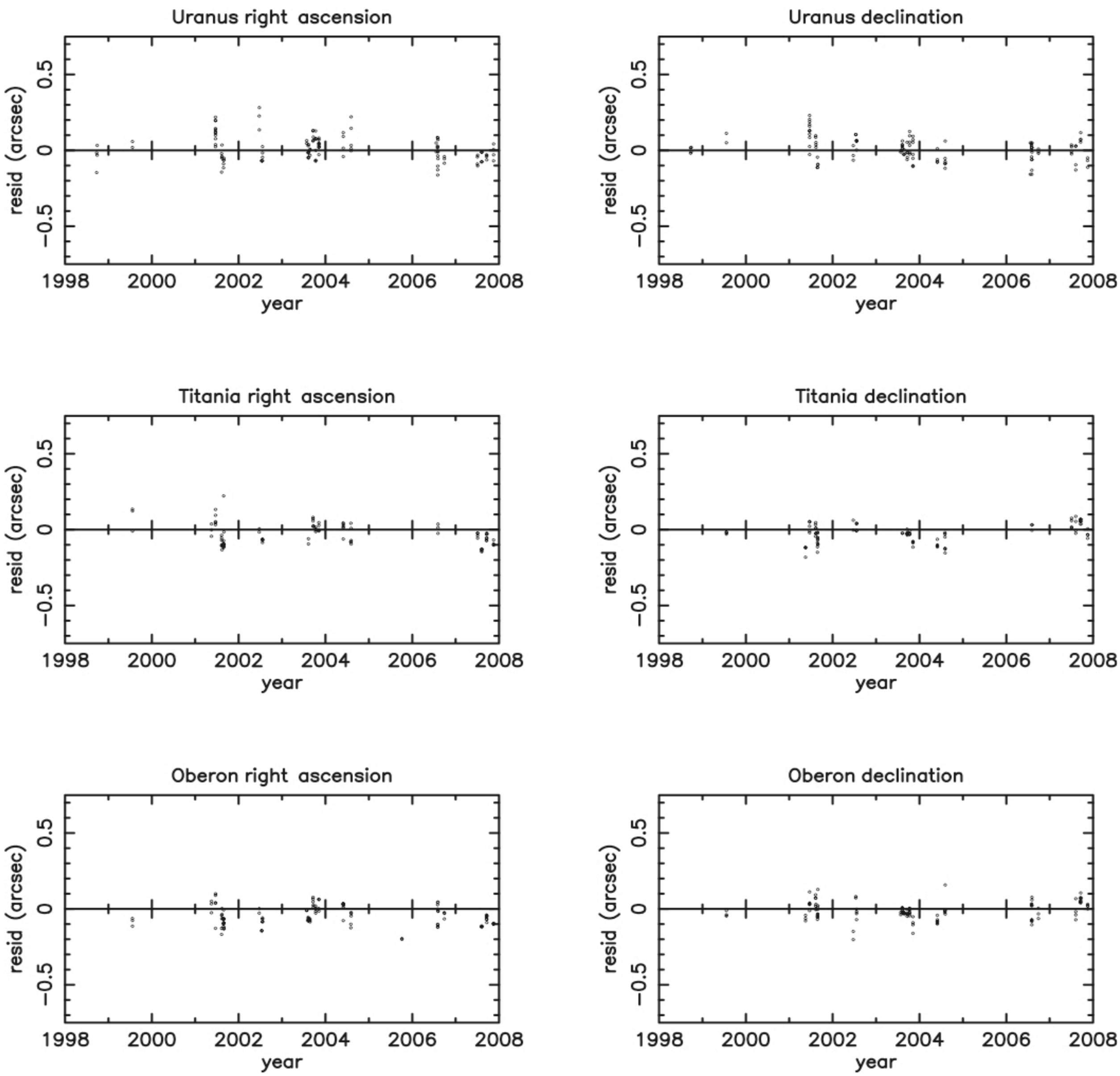

Figure B-29: Uranus observations from Table Mountain Observatory.

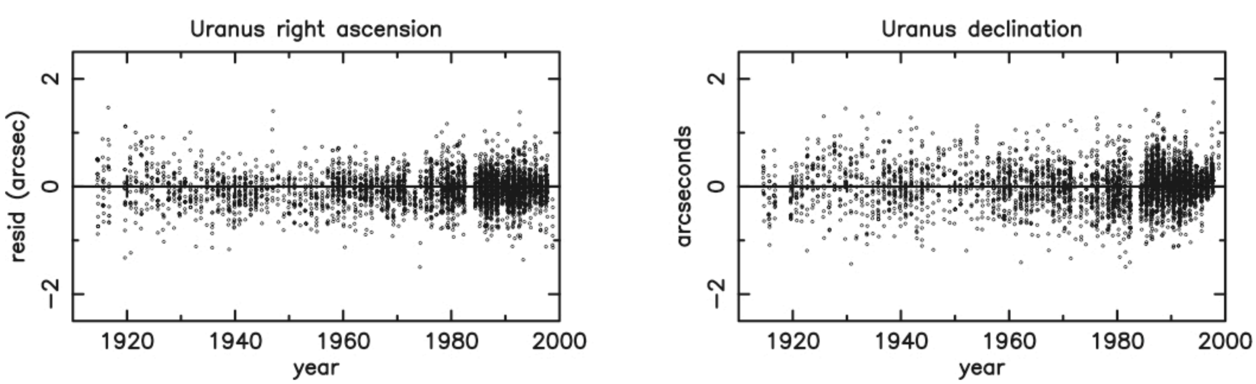

Figure B-30: Transit observations of Uranus

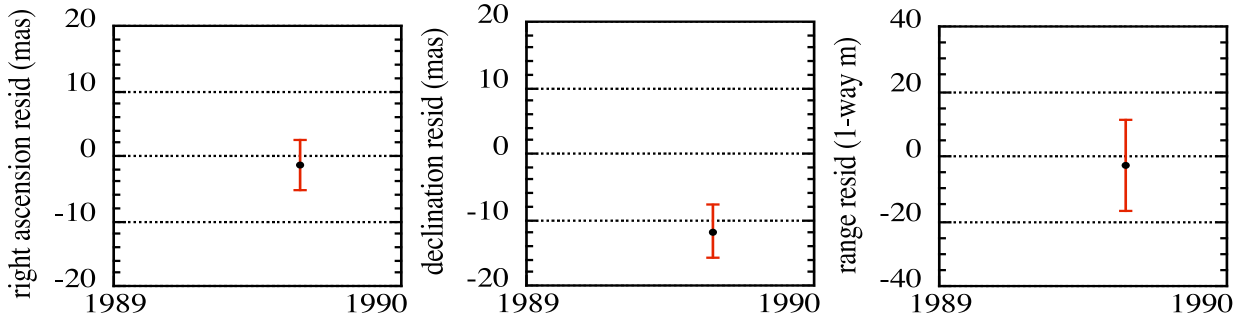

Figure B-31: Neptune right ascension, declination, and range from Voyager 2 encounter.

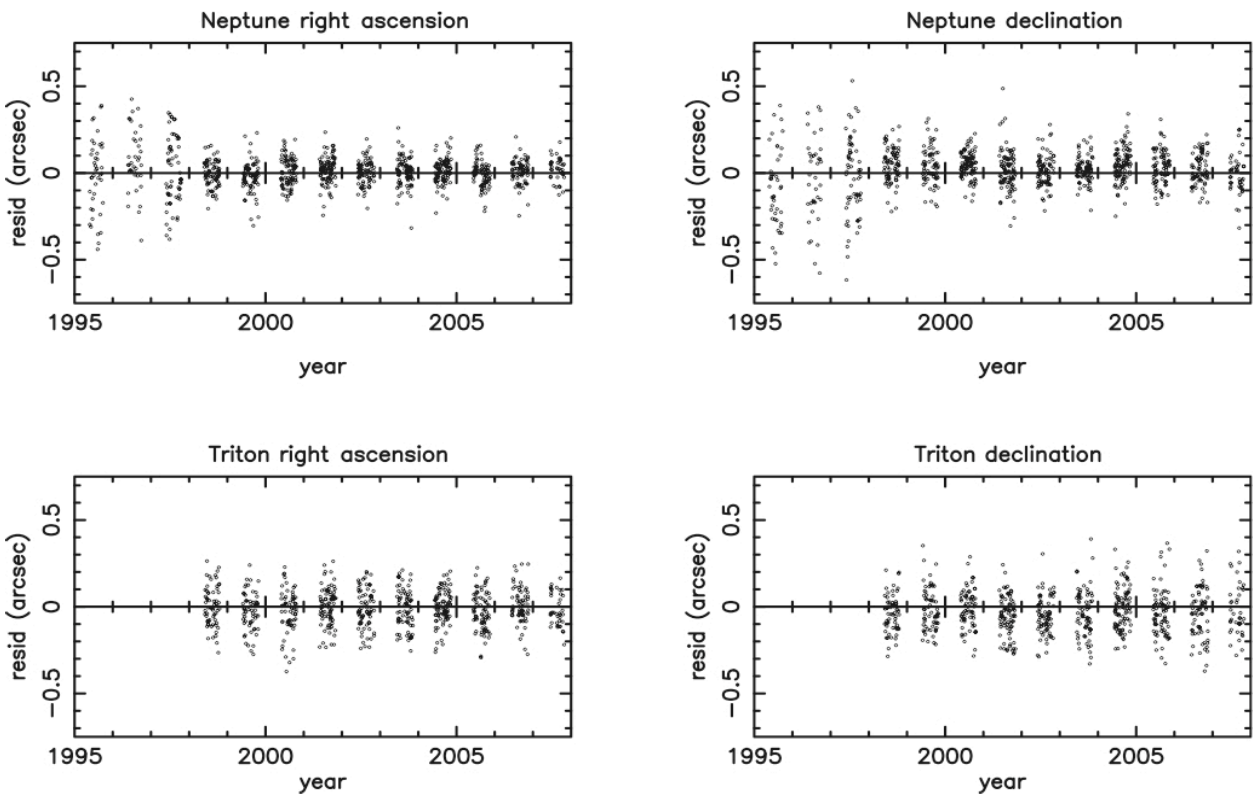

Figure B-32: Neptune observations from US Naval Observatory, Flagstaff.

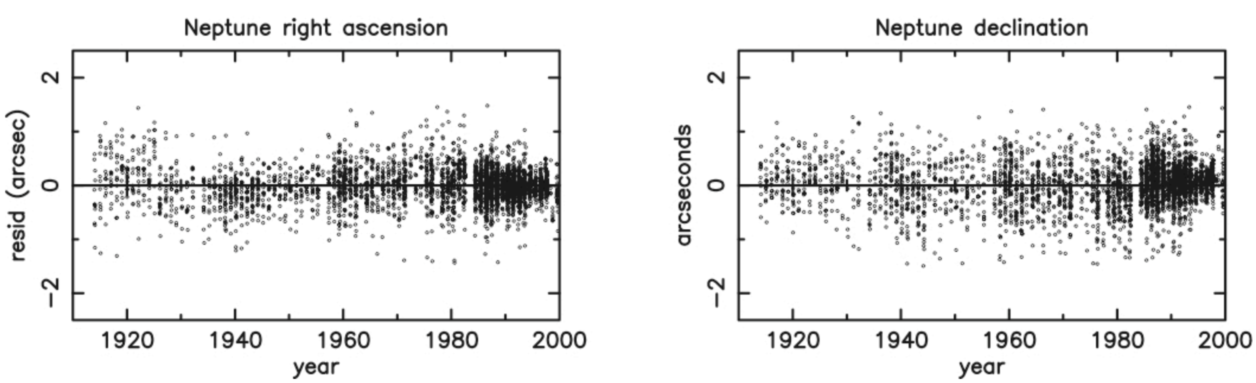

Figure B-33: Transit observations of Neptune

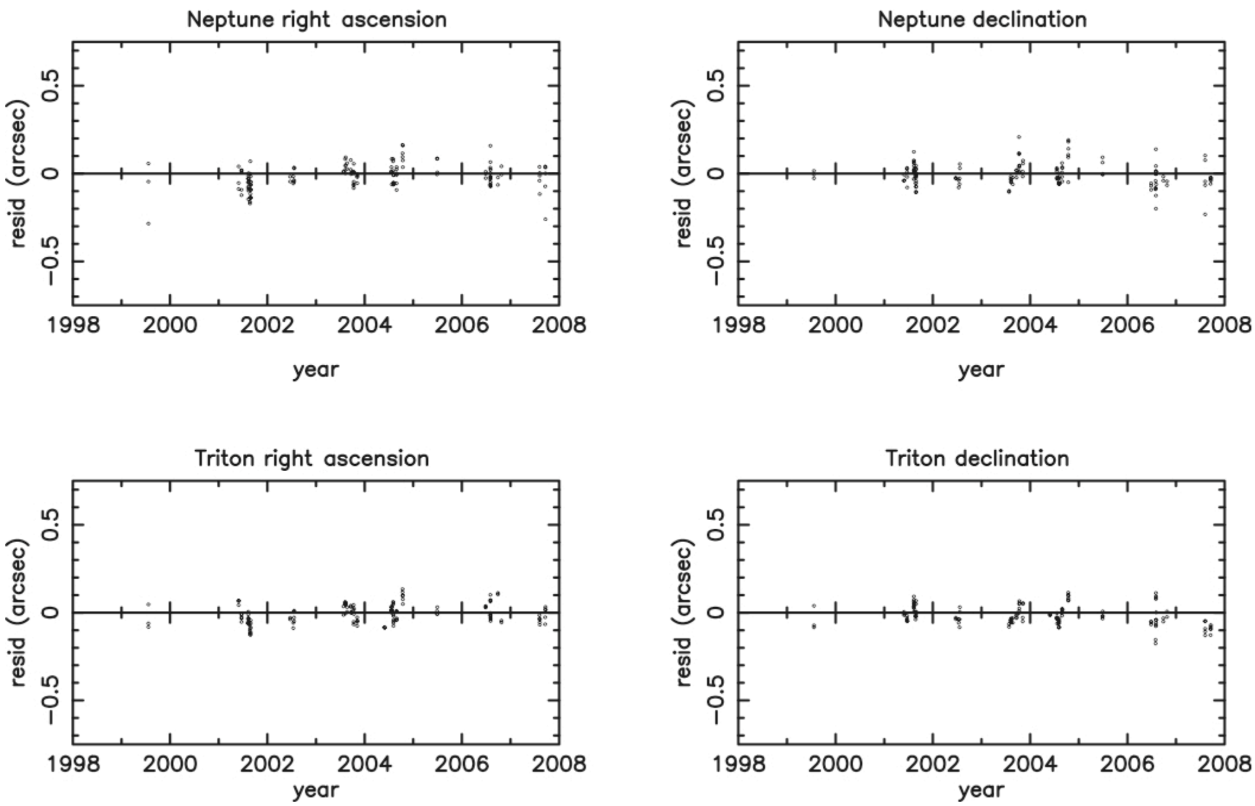

Figure B-34: Neptune observations from Table Mountain Observatory.

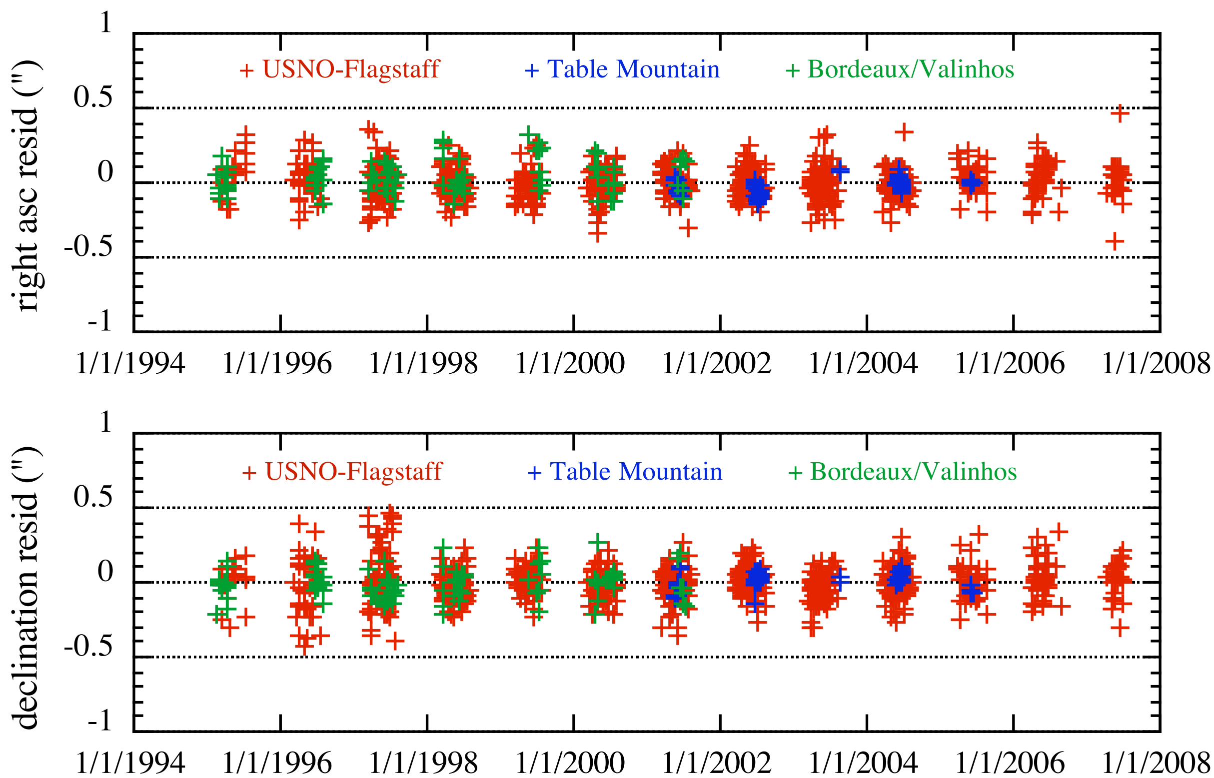

Figure B-35: Residuals of modern Pluto observations.

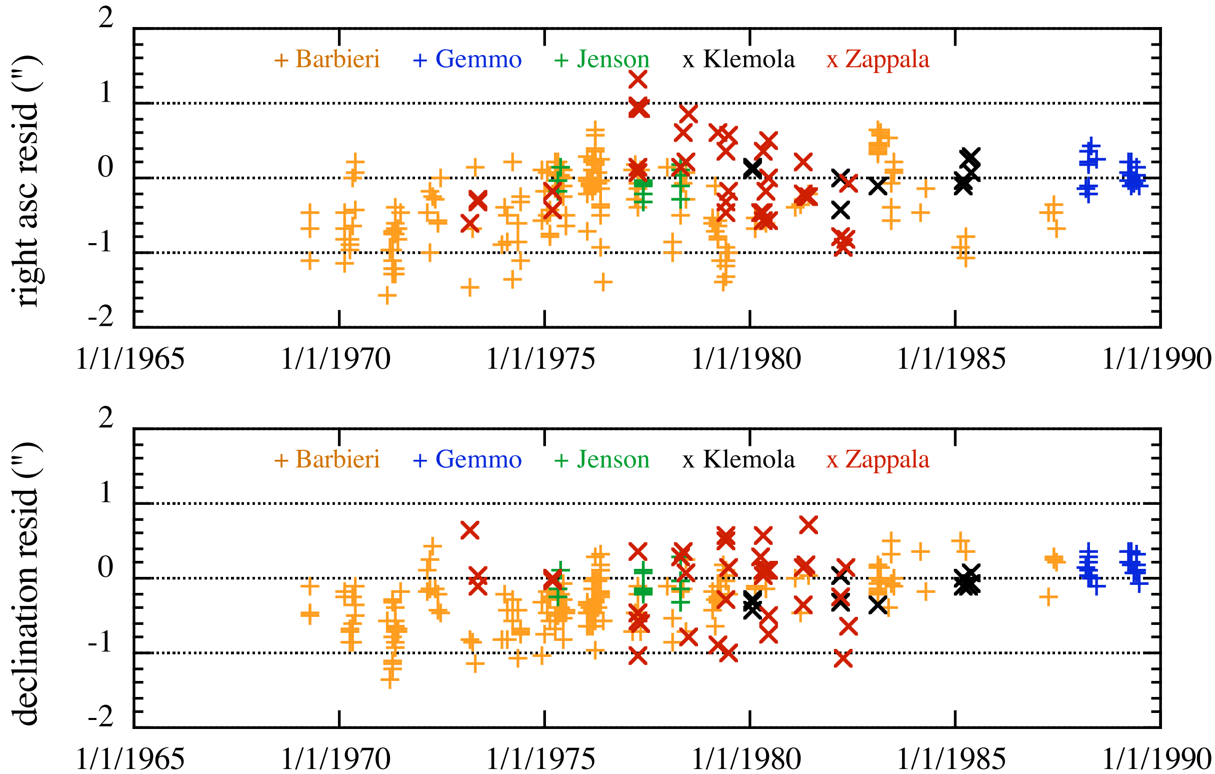

Figure B-36: Residuals of Pluto observations made 1968-1990.

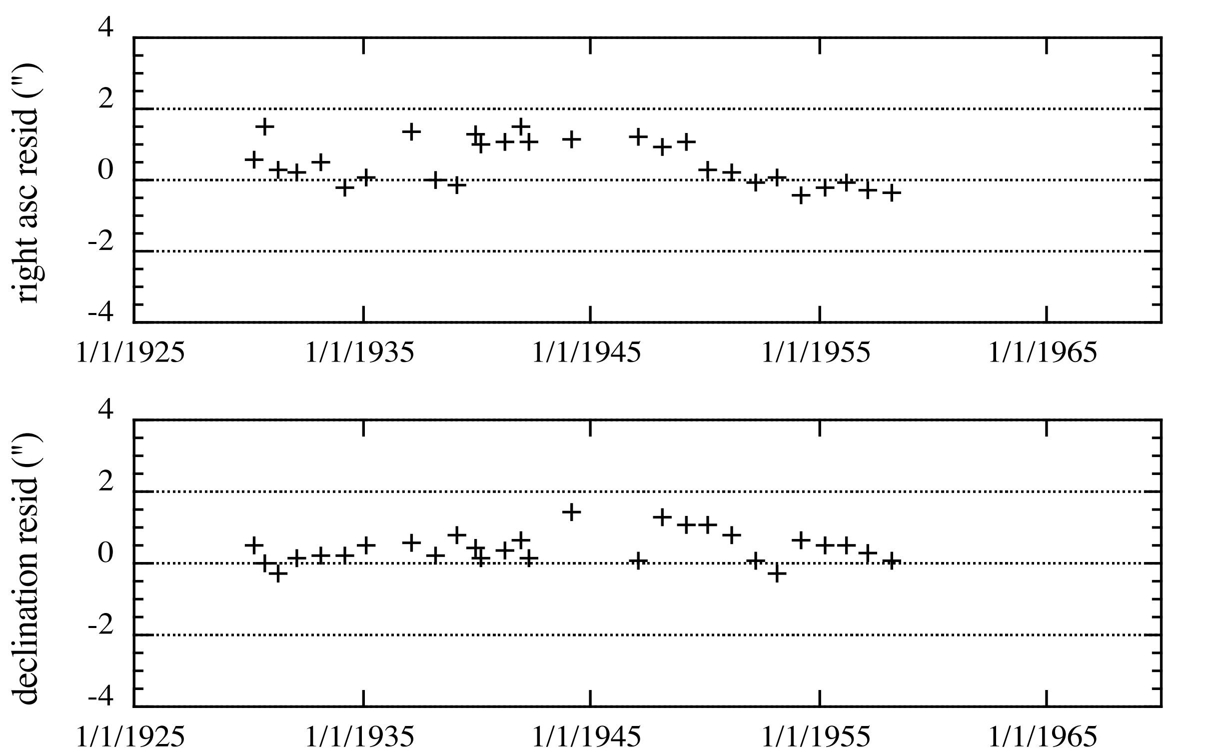

Figure B-37: Residuals of Pluto normalized points from Lowell, Yerkes, McDonald, etc.

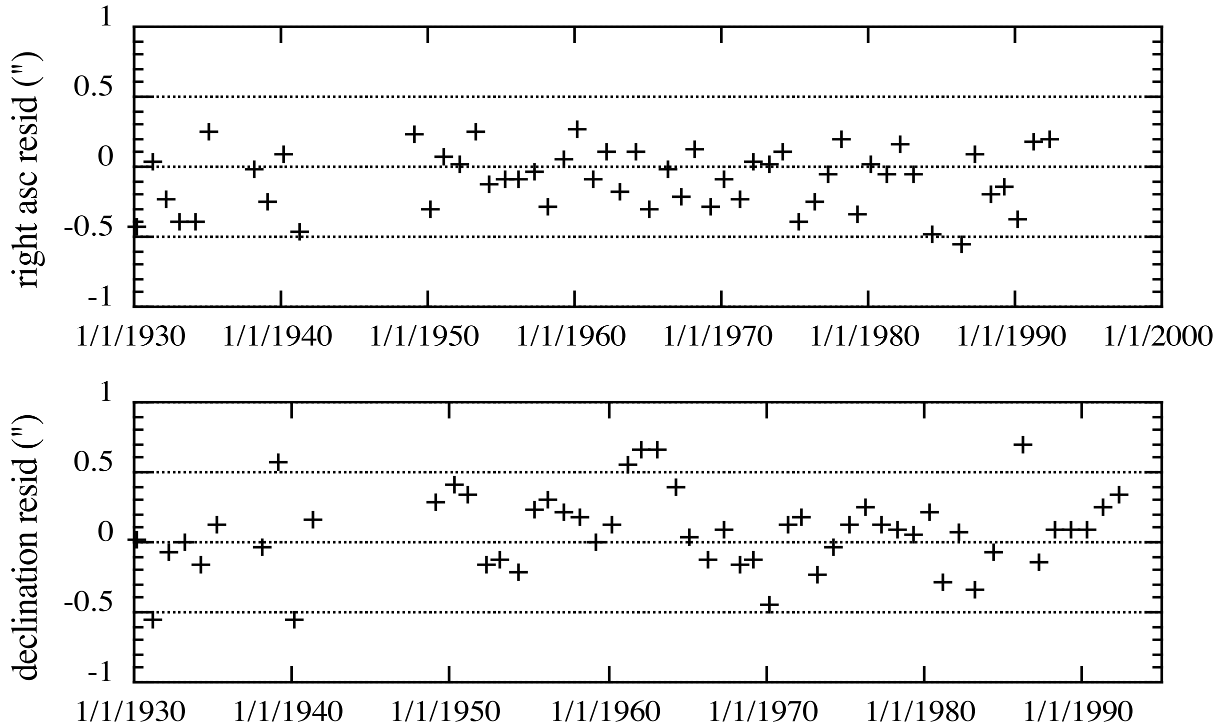

Figure B-38: Residuals of Pluto observations from Pulkovo astrograph.

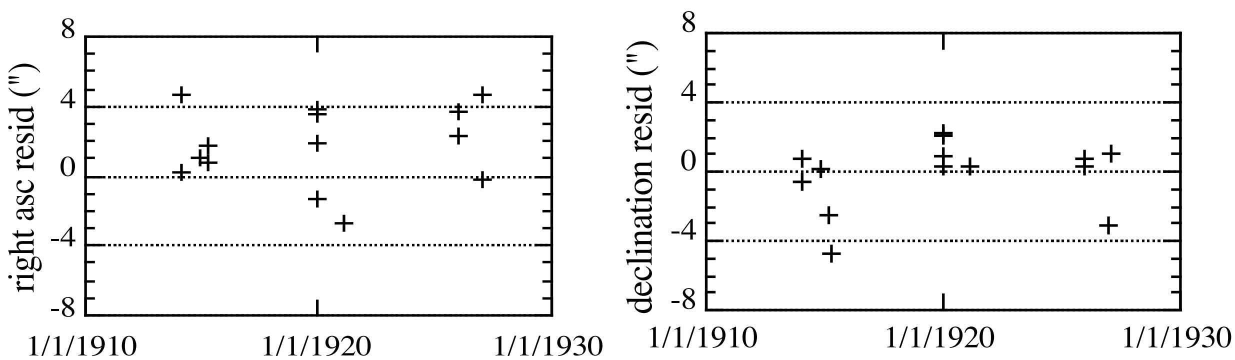

Figure B-39: Residuals of Pluto pre-discovery observations.

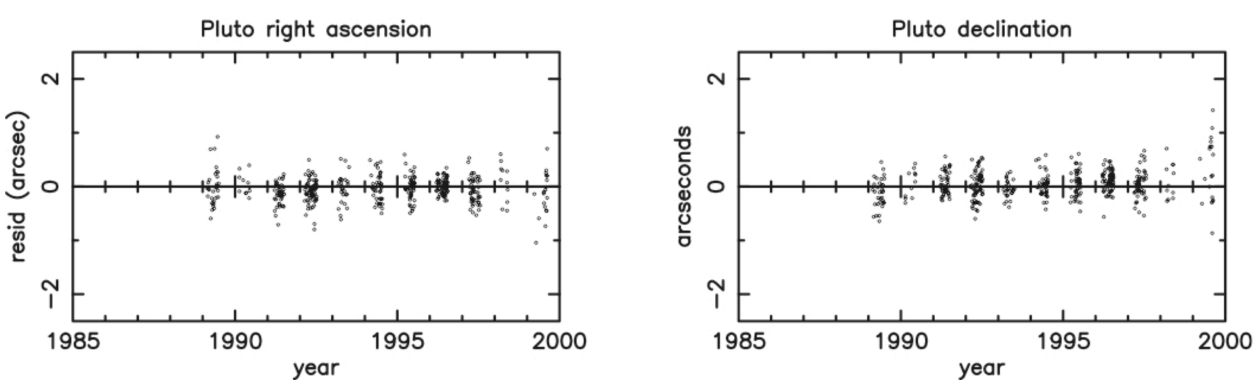

Figure B-40: Transit observations of Pluto